

SOCIETAL RESILIENCE TO FLOODING:

A CASE STUDY OF SEATTLE, WA

A Thesis

Presented in Partial Fulfillment of the Requirements for the

Degree of Master of Science

with a

Major in Geography

in the

College of Graduate Studies

University of Idaho

by

Joy D. Campbell

December 2013

Major Professor: Tim G. Frazier, Ph.D.

Authorization to Submit Thesis

This thesis of Joy D. Campbell submitted for the degree of Master’s of Science and titled “Societal Resilience to Flooding: A Case Study of Seattle,” has been reviewed in final form. Permission, as indicated by the signatures and dates given below, is now granted to submit final copies to the College of Graduate Studies for approval.

Major Professor: \_\_\_\_\_ Date: \_\_\_\_\_  
Tim Frazier, PhD

Committee Members: \_\_\_\_\_ Date: \_\_\_\_\_  
John Abatzoglou, PhD

\_\_\_\_\_ Date: \_\_\_\_\_  
Karen Humes, PhD

Geography Department Chair: \_\_\_\_\_ Date: \_\_\_\_\_  
Karen Humes, PhD

College of Science Dean: \_\_\_\_\_ Date: \_\_\_\_\_  
Paul Joyce, PhD

Final Approval and Acceptance by the College of Graduate Studies:  
\_\_\_\_\_ Date: \_\_\_\_\_  
Jie Chen, PhD

## Abstract

This study investigated how projected changes in Seattle's sea-level rise (SLR) may influence the city's resilience to flooding. Seattle's current vulnerability and resilience to SLR inundation was compared to future sea-level rise scenarios. Areas of lowest resilience were determined using the Spatially Explicit Resilience-Vulnerability Model (SERV) as well as the Geographically Weighted Spatially Explicit Resilience-Vulnerability Model (GWSERV) and a GIS overlay of Seattle's exposure to SLR. The GWSERV model provides more detailed and localized results making it more useful to stakeholders. Unlike previous models, GWSERV results allow stakeholders to direct hazard mitigation and recovery efforts to specific census blocks as well as on specific populations. Results indicate that if local climate change predictions are realized, Seattle's resilience to SLR will change very little because of the rapid change in elevation along the coastlines.

## Acknowledgments

I would like to thank the members of my committee, Dr. Tim Frazier, Dr. John Abatzoglou, and Dr. Karen Humes for their support and guidance. I would also like to thank Dr. Frazier for his patience, expertise, and support through months of modeling and setbacks. I would like to acknowledge Dr. Nathan Wood for his help acquiring data for this project and Idaho EPSCoR, ICE-Net, and the Department of Geography for funding. I would have had a much harder time with this work without my office and classmates. Their help and impromptu dance and coffee breaks are much appreciated. I would like thank Shahen Huda for his endless support, encouragement, and editing help. Finally, I would like to thank my parents and siblings for talking me through the hard times and pushing me to challenge myself.

## Table of Contents

Authorization to Submit Thesis .....	ii
Abstract.....	iii
Acknowledgments .....	iv
Table of Contents.....	v
List of Figures.....	vii
List of Tables .....	ix
Chapter 1: Introduction and Literature Review .....	1
1.1: Introduction.....	1
1.2: Study Area .....	4
1.3: Research Questions and Goals.....	7
1.4: Literature Review.....	7
1.5: Data .....	11
1.6: Analytical methods .....	12
1.7: Thesis Format.....	14
Chapter 2: Methods.....	15
2.1: Sea-Level Rise .....	15
2.2: SERV .....	16
2.3: GWSERV .....	19
Chapter 3: Results, Discussions, and Conclusions .....	24

3.1: Exposure ..... 24

3.2: SERV ..... 30

3.3: GWSERV ..... 40

3.4: SERV vs. GWSERV ..... 69

3.5: Discussions and Conclusions ..... 70

References ..... 78

## List of Figures

Figure 1: Study Area.....	5
Figure 2: Seattle Population Density Map.....	6
Figure 3: 0.010 Exposure Map .....	26
Figure 4: 0.105 Exposure Map .....	27
Figure 5: 3.804 Exposure Map .....	28
Figure 6: 4.610 Exposure map.....	29
Figure 7: SERV: Adaptive Capacity Result map .....	32
Figure 8: SERV: Sensitivity Results map.....	35
Figure 9: SERV: 0.010 map.....	36
Figure 10: SERV: 0.105 map.....	37
Figure 11: SERV: 3.804 map.....	38
Figure 12: SERV: 4.610 map.....	39
Figure 13: GWSERV: Adaptive Capacity Total PVE map.....	41
Figure 14: GWSERV: Adaptive Capacity Component 1 map .....	42
Figure 15: GWSERV: Adaptive capacity Component 1 PVE map.....	44
Figure 16: GWSERV: Adaptive Capacity Component 2 map .....	45
Figure 17: GWSERV: Adaptive Capacity Component 2 PVE map.....	46
Figure 18: GWSERV: Adaptive Capacity Component 3 map .....	47
Figure 19: GWSERV: Adaptive Capacity Component 3 PVE map.....	48
Figure 20: GWSERV: Adaptive Capacity Component 4 map.....	49
Figure 21: GWSERV: Adaptive Capacity Component 4 PVE map.....	50

Figure 22: GWSERV: Adaptive Capacity Results map .....	51
Figure 23: GWSERV: Sensitivity Total PVE map.....	53
Figure 24: GWSERV: Sensitivity Component 1 map .....	54
Figure 25: GWSERV: Sensitivity Component 1 PVE map.....	55
Figure 26: GWSERV: Sensitivity Component 2 map .....	56
Figure 27: GWSERV: Sensitivity Component 2 PVE map.....	57
Figure 28: GWSERV: Sensitivity Component 3 map .....	58
Figure 29: GWSERV: Sensitivity Component 3 PVE map.....	59
Figure 30: GWSERV: Sensitivity Component 4 map .....	60
Figure 31: GWSERV: Sensitivity Component 4 PVE map.....	61
Figure 32: GWSERV: Sensitivity Results map .....	63
Figure 33: GWSERV: 0.010 map.....	65
Figure 34: GWSERV: 0.105 map.....	66
Figure 35: GWSERV: 3.804 map.....	67
Figure 36: GWSERV: 4.610 map.....	68
Figure 37: Seattle Elevation.....	71
Figure 38: 3.804 Comparison .....	72

## List of Tables

Table 1: SLR Scenarios .....	16
Table 2: Adaptive Capacity Indicators .....	22
Table 3: Sensitivity Indicators .....	23
Table 4: Number of Exposed Blocks.....	25
Table 5: Adaptive Capacity: PCA Results.....	31
Table 6: Sensitivity: PCA Results .....	33
Table 7: Count in each Vulnerability Bracket.....	69

## Chapter 1: Introduction and Literature Review

### 1.1: Introduction

Coastal communities are vulnerable to a variety of hazards including flooding, hurricanes, storm surge, and sea-level rise (SLR) (Wisner, Blaike, Cannon, & Davis, 2004). Natural hazards occur where human life and the environment interact (Wisner et al., 2004). Four hazard types; floods, tropical cyclones, earthquakes, and droughts, represent approximately 90 percent of the world's natural disasters (Burton, Kates, & White, 1978). Unfortunately areas that are the most appealing for new development, such as beachfronts, river shores, and mountainsides, are often the most hazardous. The threat of hurricanes, floods, and landslides does little to discourage development in these hazardous areas. In many cases, changes to public policy also does little to dissuade development in these areas (Godschalk, Brower, & Beatley, 1989). Today, about 10 percent of global population resides in low elevation coastal zones (less than 10 meters in elevation). This population is on only 2 percent of the world's land (Department of Economic and Social Affairs, 2011). In the United States, between 1970 and 2010, coastal communities increased in population by about 40 percent, and today 39% of the US population lives in counties that are adjacent to the coast (US Department of Commerce National Oceanic and Atmospheric Administration, 2012).

SLR is a geophysical condition that enhances coastal community vulnerability. Global sea level, on average, rose at a rate of 1.8 mm per year between 1961 and 2003. That rate increased between 1993 and 2003 to a rate of 3.1 mm per year. Models predict an eustatic sea-level change of between 0.18 m and 0.59 m by 2099, however that range can

vary locally due to local factors such as bathymetry, tides, and isotactic rebound of the continental plate (Bernstein et al., 2007). SLR increases communities' vulnerability to flooding as well as coastal storms by exposing more infrastructure to the water (Cooper, Chen, Fletcher, & Barbee, 2012; Frazier, Wood, Yarnal, & Bauer, 2010a; Kleinosky, Yarnal, & Fisher, 2006; Wu, Yarnal, & Fisher, 2002). Moreover, global precipitation patterns are projected to change with a likelihood of increased frequency of heavy precipitation events (Bernstein et al., 2007). SLR combined with changes in precipitation patterns could have widespread and unknown effects on local resilience and vulnerability (Frazier et al., 2010a). Other consequences of climate change could include flooding, sewer surcharge, and combined sewer overflow, exposing the areas to more hazards and thus increasing the area's vulnerability (Nie, Lindholm, Lindholm, & Syversen, 2009).

Generally, vulnerability is defined as the potential for loss (Adger, 2006; Cutter, Boruff, & Shirley, 2003; Füssel, 2006; Smit & Wandel, 2006; Turner et al., 2003), however, in this research, vulnerability will be defined as a function of a system's exposure, sensitivity, and adaptive capacity to a hazard (Frazier et al., 2010a; Polsky, Neff, & Yarnal, 2007). Exposure to the hazard is the "nature and degree to which a system experiences environmental or socio-political stress" (Adger, 2006), sensitivity is "the degree to which a system is modified or affected by perturbations" (Adger, 2006), and adaptive capacity is "the ability of a system to evolve in order to accommodate environmental hazards or policy change and to expand the range of variability with which it can cope" (Adger, 2006).

A community's resilience is heavily influenced by the community's adaptive capacity and in turn so is the vulnerability of the community to hazards (Gallopín, 2006). Although the concept of resilience was developed in regards to ecological systems, it has

evolved to include economic and social systems (Holling, 1973; Janssen, Schoon, Ke, & Börner, 2006). Resilience in regards to “social-ecological systems, is related to (i) the magnitude of shock that the system can absorb and remain within a given state; (ii) the degree to which the system is capable of self-organization; and (iii) the degree to which the system can build capacity for learning and adaptation” (Folke et al., 2002). Vulnerability and resilience research have common elements; both study the “shocks and stresses experienced by the social-ecological system, the response of the system, and the capacity of adaptive action” (Adger, 2006). In other words, as a community increases its resilience to a natural hazard, it decreases its vulnerability to the hazard. Resilience can also be seen as the capacity of the social system to react and recover to an event during and after the event, whereas vulnerability is often seen as a pre-event condition (Cutter et al., 2008b). It is also essential to note that community resilience, vulnerability, and adaptive capacity is temporal in nature and changes with the changing community (Cutter & Emrich, 2006). However, in this research it is assumed that resilience, vulnerability, and adaptive capacity are constant through time due to the scope of the project.

Community resilience to hazards is important because it allows a community to recover from larger shocks to the system and continue to be sustainable (Folke et al., 2002). Community sustainability is the ability for a community to “tolerate – and overcome – damage, diminished productivity, and reduced quality of life from an extreme event without significant outside assistance” (Mileti, 1999). Natural hazard mitigation is necessary if communities want to enhance community sustainability. Mileti suggests that in order to increase community sustainability to hazards, the community should maintain and enhance environmental quality of the local ecosystem and people’s quality of life, foster local

resiliency to disasters and a diversified local economy, ensure inter- and intragenerational equity, and have a consensus-building approach in which all stakeholders have a say in the policy and community design decisions made (Mileti, 1999). Increasing community resilience will increase the community's long-term sustainability. This research will investigate how rising sea level and changing precipitation levels will influence a community's resilience to flooding.

## 1.2: Study Area

The city of Seattle in King County, Washington is known nationwide for its proactive approach to hazards mitigation and planning in the face of climate change (Saavedra & Budd, 2009). The city's large (620,778) and growing population (2.0 percent per year) makes it a relevant location to study (US Census, 2012). Figure 1 is the study area map and Figure 2 shows the population density of Seattle. Local sea level is projected to rise 0.55 m – 1.28 m by 2100 and an increase of 1-2 percent in annual precipitation, although some models project wetter autumns and winters and drier summers (Mote & Salathé, 2010). A 2008 report conducted by the Wastewater Treatment Division (WTD) of King County determined that wastewater facilities could flood with SLR of higher than 0.8 ft (24.4 cm), within the estimated range of SLR for Puget Sound by 2100 (WTD, 2008). The WTD study was a good starting point for measuring community exposure to future flooding, however it did not investigate community vulnerability and resilience. The study used LiDAR images within a GIS to determine the current elevation of wastewater facilities, followed by a “bath-tub” model within ArcGIS to determine future sea levels. Historical tide and storm sea levels were added to future sea levels to determine the extent of SLR under

historical conditions (WTD, 2008). This research expanded on the WTD study by integrating societal aspects of resilience and vulnerability with SLR into the study.

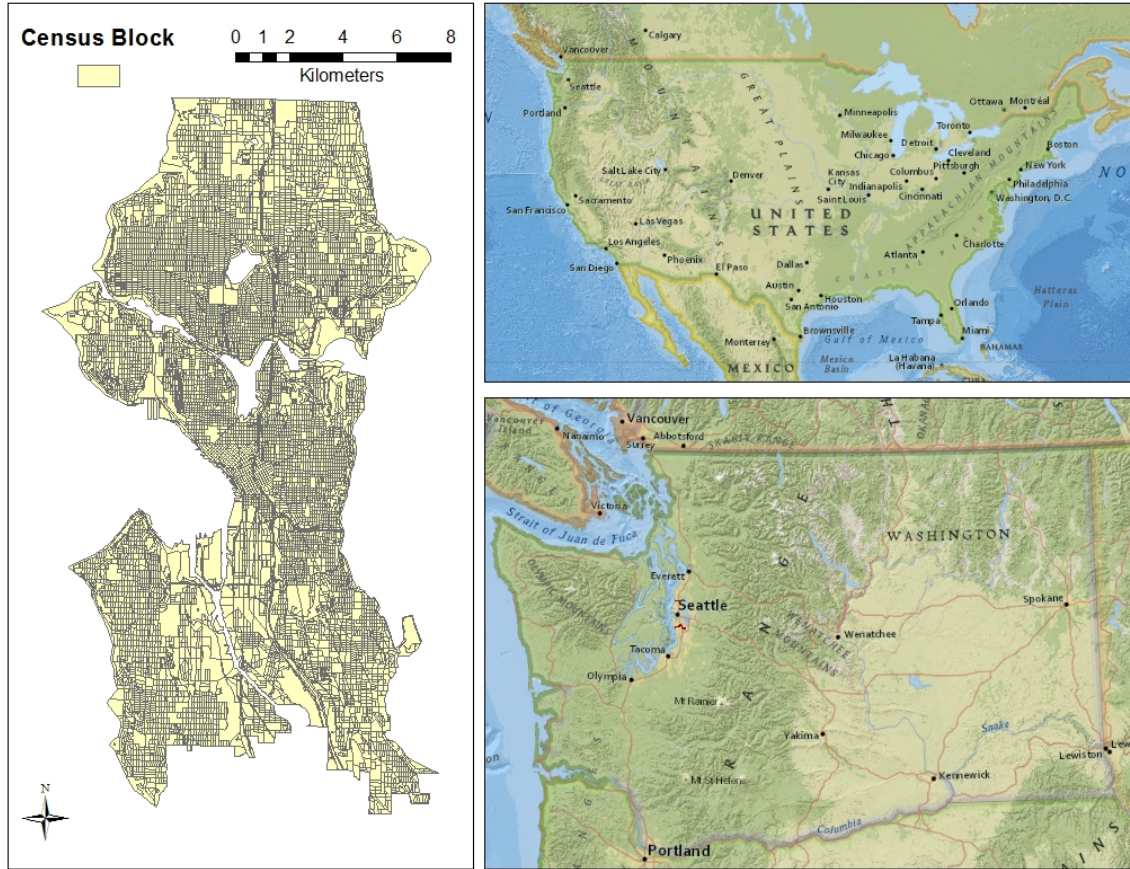
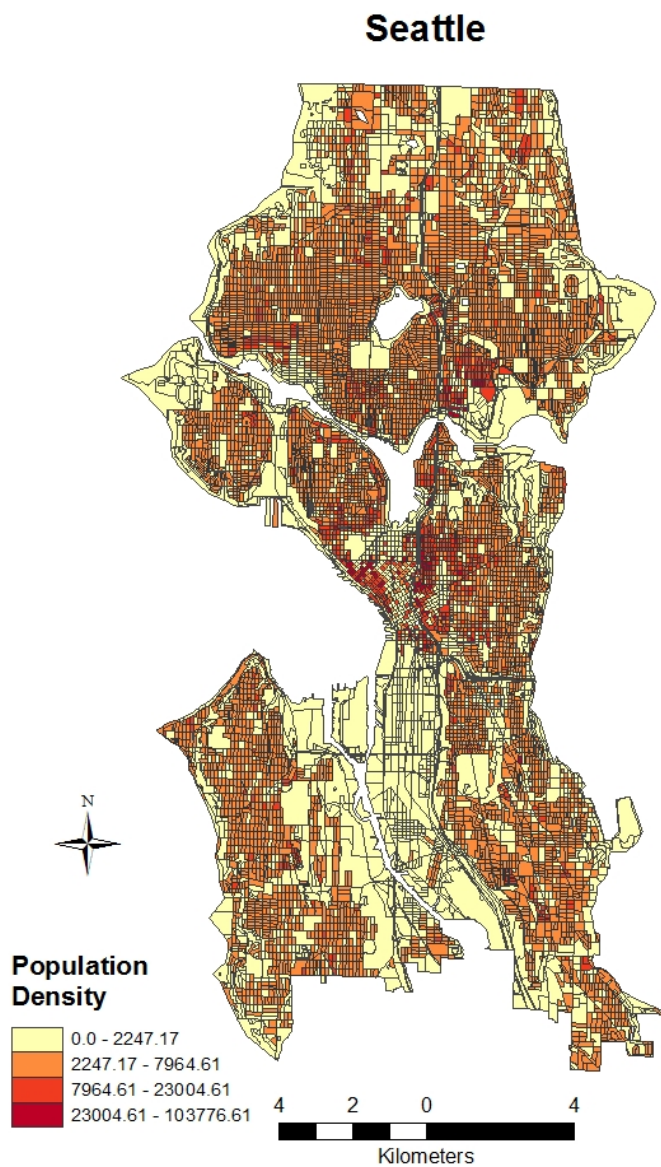


Figure 1: Study Area



**Figure 2: Seattle Population Density Map**

### 1.3: Research Questions and Goals

The goal of this research is to examine coastal community resilience to future flooding. The following questions will be addressed in this research:

- What impacts will SLR have on inundation for coastal Seattle?
- What are the benefits and constraints of using localized spatial analysis techniques towards the development of resilience quantification frameworks?

### 1.4: Literature Review

Community resilience to hazards can be measured by a variety of indicators, however, these indicators are generalizations that cannot capture every nuance of reality and are flawed (Birkmann, 2007). For example, indicators are often chosen based on data availability, which can exclude important indicators of vulnerability. Data may not be available at the scale necessary for the project and downscaling or upscaling methods could insert error into the index (Birkmann, 2007). Many indices rely on comparing communities with other communities, which can lead to a false sense of resilience, when, in fact, an entire region is in need of improvements (Birkmann, 2007).

Physical, social, political, economic, institutional and ecological components all influence vulnerability and resilience (Cutter et al., 2008b). Cutter et al. developed a resilience baseline assessment that integrates four metrics: social vulnerability, built environment and infrastructure, natural systems and exposure, and hazards mitigation and planning (Cutter et al., 2008b). Cutter's Community and Regional Resilience Initiative (CARRI) framework as a starting point to determine community resilience to natural disasters and Cutter et al. suggest that that the Social Vulnerability Index (SoVI) should be

used to determine the social vulnerability of the community to natural hazards. Although the SoVI can be improved (Tate, Cutter, & Berry, 2010; Tate, 2012a), it is widely used by the Federal Emergency Management Agency (FEMA) and other governmental organizations. In spite of SoVI's wide use, significant improvements can be made. For example, SoVI is not sensitive to changes in scale, location, and variable selection (Tate, 2012a). SoVI does also does not take into account spatial variations within the indicators or the populations in question, nor does it take into account temporal aspects of vulnerability and resilience (Frazier, Thompson, & Dezzani, 2013a, 2013b).

This research will use the Spatially Explicit Resilience-Vulnerability Model (SERV) developed at the University of Idaho to as a basis to estimate Seattle's vulnerability to SLR. The SERV model works to address issues that are often raised in SoVI by making the model place specific. This is done by integrating spatial autocorrelation between the variables and choosing variables that are scale and location specific into the model (Frazier, Thompson, & Dezzani, 2013a, 2013b). This research will estimate the extent of the hazard within the community to the hazard by using a geographic information system (GIS).

Because it is nearly impossible to directly measure the components of indices are often used. For example, Wood et.al 2010 expanded on SoVI by adapting it to the census-block level instead of the county level. In order to determine the social vulnerability of Oregon census-blocks within the tsunami-inundation zone they used the original 42 SoVI variables as well as 29 new variables chosen for the census block level then ran a principle component analysis (PCA) to estimate the variance between each block. The variables included those related to, age, employment, gender, housing, race and ethnicity, and socioeconomic status. Their analysis revealed that the following 11 components explained

64.6% of the variability between the blocks: Wealth and education, age and tenancy, urban/rural, housing, labor force participation, immigration and female workers, median rent, females and nursing homes, female-headed households, and African-Americans, and Asians (Wood, Burton, & Cutter, 2010).

Wood et.al 2010's indices were based off Cutter 2000's indices and Morrow 1999's risk factors. Morrow identified the following groups as at higher risk groups, in part because of limited access to resources (Morrow, 1999).

- residents of group living facilities
- elderly, particularly frail elderly
- physically or mentally disabled
- renters
- poor households
- women-headed households
- ethnic minorities (by language)
- recent residents/immigrants/migrants
- large households
- large concentrations of children/youth
- the homeless
- tourists and transients

Most vulnerability studies continue to use indices based on the previous risk factors (Cutter et al., 2003; Cutter, Burton, & Emrich, 2010; Frazier, Thompson, Dezzani, & Butsick, 2013; Frazier, Thompson, & Dezzani, 2013a; Frazier et al., 2010a; Wisner et al., 2004; Wood et al., 2010).

Factor analysis, specifically PCA, are widely used in the literature (Broad, Campbell, Frazier, Howe, & Murtinho, 2010; Cutter et al., 2003; A. Fekete, 2009; Alexander Fekete, 2011; Frazier, Thompson, & Dezzani, 2013a, 2013b; Frazier et al., 2010a; Tate et al., 2010; Wood et al., 2010). For example, Cutter et al. tested for multicollinearity between each of the 250 variables that they collected and found a subset of 85 raw variables. The data was

then normalized to percentages, per capita, or density function. The 85 variables were reduced to 42, then to 11 using PCA at each step. They used a varimax rotation and chose the 11 factors with eigenvalues that were higher than 1.00 (Cutter et al., 2003). Wood et al. 2010 expanded on the SoVI by using it at a smaller scale, the census block level instead of the county level, however they followed the same methods as Cutter et al did in 2003 (Wood et al., 2010). Alexander Fekete developed a Social Vulnerability Index (SVI) that also uses PCA as well as logistic regression to determine vulnerability scores. However, in some cases, vulnerability indices are not aggregated statistically, but instead assigned a score and added to create score out of 100 (Mustafa, Ahmed, Saroch, & Bell, 2011).

Although traditional PCA and other data aggregation methods are useful, they do not take into account spatial autocorrelation between the indices at whatever scale they are used at. The SERV model, developed by Frazier et al. 2013, integrates spatial autocorrelation into the social vulnerability model (Frazier, Thompson, & Dezzani, 2013a, 2013b). To integrate spatial autocorrelation into the SERV model, Frazier et al. first conducts a Moran's I on every indicator to determine if spatial autocorrelation is significant to 5%. Researchers then conducted a PCA on the indicators and utilized a gamma rotation instead of a varimax rotation because the indicators were determined to be spatially autocorrelated and thus not independent. Different indicators were chosen to determine adaptive capacity and the same statistical methods were followed. Frazier et al. then aggregated the sensitivity score along with exposure and adaptive capacity score to estimate the vulnerability of each census block (Frazier, Thompson, & Dezzani, 2013a; Thompson, 2012). Frazier et al.'s study was one of the first to take into account spatial autocorrelation between indicators at a census block level as well as assign different weights to each indicator. The SERV model then aggregates

the exposure, sensitivity, and adaptive capacity to the hazard to create a vulnerability score. The PCA was done for both sensitivity and adaptive capacity to the hazards. Although the SERV model integrates spatial autocorrelation between the variables by using a gamma rotation instead of a traditional varimax rotation, it does not include any geographic weights in the computation.

Demšar et al. 2013, details the different ways that PCA can be used spatially. For example, one can run a PCA on spatial objects or raster data without including geography in the computation. However, one can also include spatial effects in the PCA by using a locally weighted PCA (LWPCA) or a geographically weighted PCA (GWPCA). LWPCA and GWPCA are applied to data where different locations or regions of data may require different PCs (Demšar, Harris, Brunson, Fotheringham, & McLoone, 2013). GWPCA is used when the distances between the regions are determined by geographic distance and local eigenvalues are used for data reduction. Unfortunately, there is no diagnostic test to see if GWPCA offers any advantages over a global PCA (Demšar et al., 2013)..

## 1.5: Data

In order to estimate the resilience of Seattle to SLR, exposure, sensitivity, and adaptive capacity data will be needed. Using existing literature, local SLR will be estimated in order to provide future scenarios of exposure to flooding for Seattle (Committee on Sea Level Rise in California, Oregon et al., 2012; P. Mote et al. 2008; Bernstein et al. 2007). Historical tide data as well as current climate conditions will be acquired to set a baseline for future changes. A current LIDaR derived digital elevation model (DEM) will be used to supplement the GIS data by determining the elevation of the community. ArcGIS will be

used to determine the extent of SLR, combined with high tide, to determine where the community may be inundated in the event of a storm.

After determining hazard extents, community exposure to flooding will then be determined in each scenario. Each hazard scenario will be overlaid with community boundaries to determine the exposure of the community to flooding by using ArcGIS. This will be done to determine the extent of exposure of community societal assets such as, infrastructure, residential population, businesses etc. US Census 2010 data, as well as economic data from Info USA (2011), will be used to determine the social vulnerability to hazards using the SERV model. Because the lowest spatial unit that population data is collected at in the US is at the census block level, the economic data will be aggregated to that level. In cases where the lowest aggregation of data is the census tract level, the data will be averaged to the block.

#### 1.6: Analytical methods

The statistical methods that will be the focus of this project are on the estimation of Seattle's societal resilience to climate change. The methods that will be used will follow the SERV model that was developed by Frazier et al. 2013 because, unlike previous vulnerability and resilience models, it integrates spatial autocorrelation and better integrates scale into the model (Frazier, Thompson, & Dezzani, 2013a, 2013b; Thompson, 2012). This research will follow the SERV model and then slightly alter the SERV model by integrating special effects into the model by using GWPCA on the adaptive captivity and sensitivity indicators. The original SERV model will be referred to as "SERV" and the geographically weighted SERV model will be "GWSERV." The researcher will then determine the best

indicators to represent Seattle's resilience by using the top four components in the GWSERV model and indicators with eigenvalues over 1.00 in the SERV model. This approach is consistent with those in the literature (Cutter et al., 2003; A. Fekete, 2009; Alexander Fekete, 2011; Frazier, Thompson, & Dezzani, 2013a, 2013b; Frazier, Wood, Yarnal, & Bauer, 2010b; Christopher D. Lloyd, 2010; Tate, 2012b; Thompson, 2012; Wood et al., 2010). Exposure will be determined using a GIS overlay on each census block (Cutter et al., 2008b, 2003; Cutter, Mitchell, & Scott, 2000; Frazier, Thompson, & Dezzani, 2013a, 2013b; Frazier et al., 2010a; Thompson, 2012; Wood et al., 2010), however the probability of exposure will not be estimated because it is outside of the scope of the project. Exposure, sensitivity, and adaptive capacity will be aggregated using Equation 1 from Frazier et al. 2013a, 2013b,

$$V = [E + S] - AC$$

**Equation 1**

where V= vulnerability, E= exposure, S= sensitivity and AC= adaptive capacity (Frazier, Thompson, & Dezzani, 2013a, 2013b; Thompson, 2012). Exposure will be estimated by calculating the ratio of the area of the census block exposed to the hazard to the area not exposed. The resulting percentage will be converted to a Z-score and included in equation 1. Both sensitivity and adaptive capacity scores will be calculated by doing a PCA on the socioeconomic variables suggested in the literature and available in census block data. Variables with a loading of lower than -0.45 and higher than 0.45 will be retained in each component. Components will be retained if they have an eigenvalue of over 1.0 in the calculation of each component (Cutter et al., 2000; Frazier, Thompson, & Dezzani, 2013b). The sensitivity and adaptive capacity scores will be calculated by computing a linear

combination of principle components, weighted by their respective loadings and percent variance explained,. More detail in the score computation is provided in section 2.2.

Because resilience is temporal, future work can be done to determine how to best adapt the SERV model to represent resilience instead of vulnerability.

The null hypothesis of this study is that none of the indicators are spatially dependent (Moran's  $I = 0$ ) and each census block will exhibit similar resilience values. The alternative hypothesis is that the vulnerability indicators are spatially dependent (Moran's  $I$  is  $-1 \leq I \leq 1$  but  $I \neq 0$ ) and that the resilience values of each census block will be statistically different at 5%. By testing these hypotheses, it will be possible to answer the research questions because the SERV model will quantify the effects of climate change on the flooding potential of Seattle, the resilience of Seattle, as well as the adaptive capacity of the city to flooding.

### 1.7: Thesis Format

This thesis is formatted as follows. Chapter one is an introduction, overview, and literature review of the research. Chapter two describes the methodology used in the research. The final chapter, three, describes and discusses the results of the research, lists the limitations and areas of future study of the research, and gives concluding statements.

## Chapter 2: Methods

The goal of this research is to estimate Seattle's vulnerability and resilience to SLR. The exposure to SLR is estimated using a "bath tub" model in ArcGIS, then combined with the social vulnerability and resilience scores for Seattle. The vulnerability scores are calculated using the SERV model that utilizes PCA. The SERV model is then altered to include a GWPCA instead of a traditional PCA and becomes the GWSERV. The outcomes of both models are then compared to see if any significant differences are present.

### 2.1: Sea-Level Rise

Potential sea-level rise (SLR) was estimated using the methodology developed by Frazier et al., (2010). In order to calculate the percentage of the block exposed to inundations, an overlay analysis in ArcGIS is used (Frazier et al., 2010a). In order to estimate SLR elevations for Seattle, This research uses LIDaR DEM data collected from the Puget Sound LIDaR Consortium in 2000 to estimate the SLR elevations. The DEM was then lowered to show potential inundation due to SLR. The exposure analysis assumed that sea-level would rise at the same rate in every location irrespective of bathymetry and other geophysical considerations.

The scenarios in Table 1 were chosen based on the estimates in the 2012 study, "Sea-Level Rise for the Coasts of California, Oregon, and Washington: Past, Present, and Future" (Committee on Sea Level Rise in California, Oregon, and Washington, Board on Earth Sciences and Resources and Ocean Studies Board, & Division on Earth and Life Studies, 2012). The 2030, 2050, and 2100 scenarios are the low, mean, and high SLR estimates for

the area from the study. Each of the three estimates are added to the highest tide on record from December 17, 2012 at 3.699 m using the North American Vertical Datum of 1988 from NOAA's Tides and Currents data set.

<b>SLR Elevation Scenarios (m)</b>						
<b>Year</b>	<b>Low</b>	<b>Low + Tide</b>	<b>Mean</b>	<b>Mean + Tide</b>	<b>High</b>	<b>High + Tide</b>
<b>2030</b>	0.01	3.709	0.066	3.765	0.122	3.821
<b>2050</b>	0.061	3.76	0.105	3.804	0.271	3.97
<b>2100</b>	0.325	4.024	0.618	4.317	0.911	4.61

**Table 1: SLR Scenarios**

## 2.2: SERV

The goal of a PCA is to reduce the quantity of a large number of correlated variables into a few, uncorrelated variables while retaining most of the variation that was present in all of the individual variables (Jolliffe, 2002). The results of a PCA, the components, explained variance, and component loadings, are used to describe phenomena. PCA was first introduced in the early 1900's and has been used broadly, including in the discipline of geography. For example, researchers in geography have used PCA and factor analysis in their work. In the natural hazard research, PCA is used to help determine the leading factors of social vulnerability and resilience (Cutter et al., 2008a, 2003; Frazier, Thompson, & Dezzani, 2013a, 2013b; Frazier et al., 2010a; Schmidlein, Deutsch, Piegorsch, & Cutter, 2008; Wood et al., 2010). However, PCA is a global analysis and summarizes the data for a whole region into a single-value. It is also spatially limited and tends to emphasize

similarities across space (Charlton, Brunson, Demšar, Harris, & Fotheringham, 2010; Frazier, Thompson, & Dezzani, 2013b).

The SERV model, developed by Frazier et al. (2013a, b), is a global PCA model that integrates geographic variability by including a measurement of spatial autocorrelation, Moran's I. Since not all locations are identical, and external influences vary between locations, it is important to integrate spatial effects into PCA. Each scale of analysis also offers different insights. In other words, there is inherent spatial variation in most geographic data and it is essential to account for it. Results from one system rarely, if ever, can be replicated in another system and the process may not be stationary (Fotheringham, Brunson, & Charlton, 2002; Haining, 2003). For example, in SoVI, a global and not place specific PCA, the vulnerability components with highest explained variance will be the same no matter where the study site is. On the other hand, with a place and scale specific model like SERV, the components with the highest explained variance will vary based on the location and scale of the study area (Frazier, Thompson, & Dezzani, 2013a, 2013b).

The SERV model assumes that vulnerability (V) is a function of exposure (E), sensitivity (S), and adaptive capacity (AC). This research uses two lists of indicators chosen from historical studies (Frazier, Thompson, & Dezzani, 2013b) for adaptive capacity (Table 2) and sensitivity (Table 3) aggregated at the census block and census tract level, respectively. The indicators are converted to percentage of block population when necessary. The SERV model uses a Moran's I computation of the sensitivity and adaptive capacity indicators to determine the amount of spatial autocorrelation within the variables (Frazier, Thompson, & Dezzani, 2013a). The average Moran's I value for both sensitivity and adaptive capacity is then integrated into the PCA as the value for the Gamma rotation.

Block level vulnerability is then determined as  $V = (E + S) - AC$  (Frazier, Thompson, & Dezzani, 2013a, 2013b). The exposures are determined using an overlay analysis to estimate the percentage of each census block exposed to the hazard then converted to Z-scores.

Exposure to SLR is estimated by creating DEMs, inundating them with SLR by lowering the DEM in relation to sea level, and creating inundation maps. The inundation maps are then overlaid on the census blocks to estimate the percentage of each block exposed to SLR. The resulting percentages are converted to Z-Scores then included in the vulnerability equation.

The S and AC scores are estimated by calculating the percentage of each variable within each block. The weighted scores are then determined based on the influence of each indicator and its factor on S or AC. The raw, weighted S and AC scores are calculated using equation 2 and 3

$$S_{ik} = \sum D_{ij}L_{ik}$$

**Equation 2**

$$B_{ik} = \sum S_{ij}F_{if}$$

**Equation 3**

where  $S_{ik}$  is the weighted score of observation i on component k,  $D_{ij}$  is the value of the observation for the variable,  $L_{ik}$  is the loading of variable j on component k,  $B_{ik}$  is the sensitivity or adaptive capacity score of the block, and  $F_{if}$  is the amount of variance explained by factor f (Thompson, 2012). The variables were retained if the loading score's absolute value was greater than 0.45. The retained components were chosen if they had an eigenvalue of over 1.0 (Frazier, Thompson, & Dezzani, 2013b). The weighted scores are then summed to create aggregate raw S and AC scores. The raw scores are then converted to Z-scores and applied to the equation for vulnerability (Frazier, Thompson, & Dezzani,

2013a, 2013b). Each element of the vulnerability equation is converted a Z-score so that all elements are unit-less and can be added.

### 2.3: GWSERV

Fotheringham et al. developed a methodology to make PCA a local statistic by integrating geographic weights (Charlton et al., 2010; Fotheringham et al., 2002). This makes the GWPCA a local statistic that has multiple values, provides a summary at the local scale, accounts for non-stationarity, and emphasizes the differences across space by showing “hot-spots” (Fotheringham et al., 2002). This local analysis is beneficial because it provides an analysis at a higher resolution. An example of this benefit would be that local stakeholders can better target their hazard mitigation, adaptation, and recovery efforts to the areas that need it most.

Since GWPCA is a new and relatively untested method, few, if any, statistical packages are able to calculate it. Binbin Lu, Paul Harris, Isabella Gollini, Martin Charlton, and Chris Brunsdon developed and wrote a package for the statistical program R, GWModel, that includes a GWPCA function to follow Fotheringham’s methods (Lu, Harris, Gollini, Charlton, & Brunsdon, 2013). This research uses this GWModel for the GWSERV. In order to calculate the GWPCA, each location has a vector of observed variables (Charlton et al., 2010; Fotheringham et al., 2002; Harris, Brunsdon, & Charlton, 2011). The observed values are the socio-economic variables collected and the location is each census block. Assuming each location has unique coordinates, the basic model can be expanded to include geographic effects (Charlton et al., 2010; Fotheringham et al., 2002; Harris et al., 2011). In order to compute the GWPCA, a geographically weighted variance-covariance matrix

provides geographically weighted eigenvalues and eigenvectors. The product of each row of the data matrix with the corresponding geographically weighted eigenvectors, provides the geographically weighted component scores for each row (Charlton et al., 2010; Fotheringham et al., 2002; Harris et al., 2011).

The GWModel uses a distance matrix function to calculate geographically weighted points (Lu et al., 2013). The results from the distance function are then used to calculate the GWPCA. This research uses a Gaussian kernel with a bandwidth that is calculated using the GWPCA bandwidth included in the model. The bandwidth is the “size of the window over which a local PCA might apply” (Demšar et al., 2013). Essentially this is the range of values surrounding each data point that is included to make the geographic weight. One of the challenges with GWPCA is selecting a method to estimate the bandwidth. For example, a bandwidth that is too small will not capture any geographic effects and one that is too large will make the model a global one. A goodness of fit measure is utilized to estimate if the bandwidth best captures the effects of distance and space in the weighting matrix (Charlton et al., 2010; Fotheringham et al., 2002; Harris et al., 2011).

Another challenge arises when one has to interpret the results of a GWPCA because of the large number of components, component loadings, and explained variance. Essentially, a GWPCA calculates a separate PCA for each data point. A global PCA's results are  $m$  variables, components, eigenvalues, sets of component loadings, and sets of scores. However with a GWPCA the results are  $m$  variables, components, eigenvalues, sets of component loadings, and sets of scores for  $i$  locations (Charlton et al., 2010; Fotheringham et al., 2002; Harris et al., 2011). One way to interpret and display the results from a GWPCA is to create  $m$  maps showing the distribution of the results (Charlton et al.,

2010; Fotheringham et al., 2002; Harris et al., 2011; C. D. Lloyd, 2012; Christopher D. Lloyd, 2010). In this case, the results are shown on maps showing the first four components as well as the percent variance explained for each component.

This research alters the SERV model by using the GWPCA methods developed by Fotheringham (2002) in lieu of the Moran's I PCA computation to account for spatial variation in the data. The research visually compares the two models (SERV and GWSERV) and counts the number of blocks in each delineation of vulnerability (highest, high, medium, low, lowest) to note any differences in vulnerability. Tables 2 and 3 show the adaptive capacity and sensitivity indicators that are used in the research along with the range of values measured in Seattle.

<b>Adaptive Capacity Indicators</b>		
% Under 5	Percent of block population under age 5	Range: 0-50 %
% Above 65	Percent of block population above age 65	Range: 0-100 %
% Female Head of Household	Percent of block population with female head of house	Range: 0-100 %
% White	Percent of block population that is white	Range: 0-100 %
% Not White	Percent of block population that is not white	Range: 0-100 %
% Owner Occupied	Percent of block homes that are owner occupied	Range: 0-100 %
% of Total Tax Parcel Value	Percent of Seattle's total tax parcel value	Range: 0-1.0154 %
% of Total Employees	Percent of the total number of employees in Seattle	Range: 0-5.4737 %
% of Total Business Revenue	Percent of the total business revenue in Seattle	Range: 0-1.0154 %
% Below Poverty Line	Percent of block population that is below the poverty line	Range: 0-61.4 %
% Not HS Grad	Percent of block population that didn't graduate high school	Range: 0-41.2 %
% College Grad	Percent of block population that graduated college	Range: 12.9 - %
Gini Index	Measurement of inequality	Range: 0.316
% Unemployment	Percent of block population that is unemployed	Range: 0.5 -100 %

**Table 2: Adaptive Capacity Indicators**

<b>Sensitivity</b>		
% of Total Population	Percent of Seattle’s total population located in the block	Range: 0- 0.4553 %
% Female Population	Percent of block population that is female	Range: 0-100 %
% Under 5	Percent of block population under age 5	Range: 0-50 %
% Above 65	Percent of block population above age 65	Range: 0-100 %
Median age	Median age of the population in the block	Range: 0-93.5 years
% of Total Homes	Percent of Seattle’s total homes located in the block	Range: 0- 0.3001 %
% Female Head of Household	Percent of block population with female head of house	Range: 0-100 %
% White	Percent of block population that is white	Range: 0-100 %
% Not White	Percent of block population that is not white	Range: 0-100 %
% Renter Occupied	Percent of block homes that are renter occupied	Range: 0-100 %
% of Total Employees	Percent of the total number of employees in Seattle	Range: 0-2.0482 %
% of Total Business Revenue	Percent of the total business revenue in Seattle	Range: 0-1.1434 %

**Table 3: Sensitivity Indicators**

The methods described answer the research questions in the following ways. The “bath-tub” model estimates the extent that SLR might inundate Seattle, answering what impacts will SLR have on inundation for coastal Seattle. The benefits and constraints of using localized spatial analysis techniques towards the development of resilience quantification frameworks is answered by comparing the global SERV to the local GWSERV. The combination of the methodology will describe the Seattle’s resilience to SLR.

## Chapter 3: Results, Discussions, and Conclusions

Seattle's vulnerability and resilience scores were estimated using both the SERV and GWSERV models. The models were compared visually and by counting the number of blocks in each range of vulnerability. Both models require estimates of sensitivity, adaptive capacity, and exposure to SLR. Exposure was determined using a "bath-tub" model in ArcGIS. The sensitivity and adaptive capacity scores were determined using PCA (for the SERV model) and GWPCA (for the GWSERV model). The results indicate that there is no statistical difference between the SERV and GWSERV models for any of the 18 SLR scenarios. Although 18 SLR scenarios were completed, four are highlighted in the results. These four are inundations of 0.010, 0.105, 3.804, and 4.610 m, which span the range of possible results. The 0.105 and 3.804 m scenarios were chosen because they represent mean SLR estimates for 2050 with and without adjustments for high tide.

### 3.1: Exposure

Seattle's exposure to SLR was estimated using a "bath-tub" model in ArcGIS. The fraction of each 2010 Census block exposed to SLR was calculated and converted to a Z-score. The Z-scores were then input into the SERV and GWSERV models. Table 4 displays the number of exposed blocks in each scenario. Shaded scenarios include high tide.

<b>Number of Exposed Blocks</b>	
<b>SLR Scenario (m)</b>	<b># Exposed Blocks</b>
0.010	398
0.061	398
0.066	398
0.105	398
0.122	398
0.271	398
0.325	398
0.618	398
0.911	398
3.709	434
3.760	436
3.765	436
3.804	441
3.821	441
3.970	445
4.024	450
4.317	457
4.610	536

**Table 4: Number of Exposed Blocks**

Figures 3, 4, 5, and 6 show the fraction of each block exposed to SLR.

**Scenario: 0.010 (m)  
Exposure**

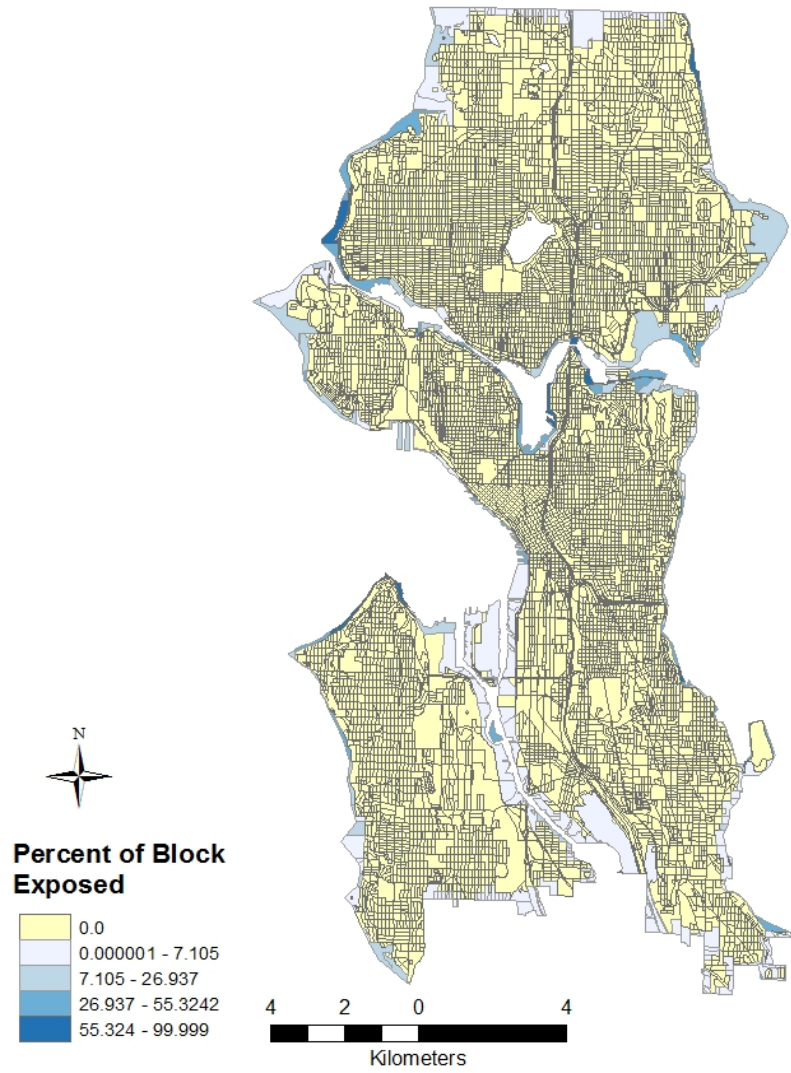


**Figure 3: 0.010 Exposure Map**

### Scenario: 0.105 (m) Exposure

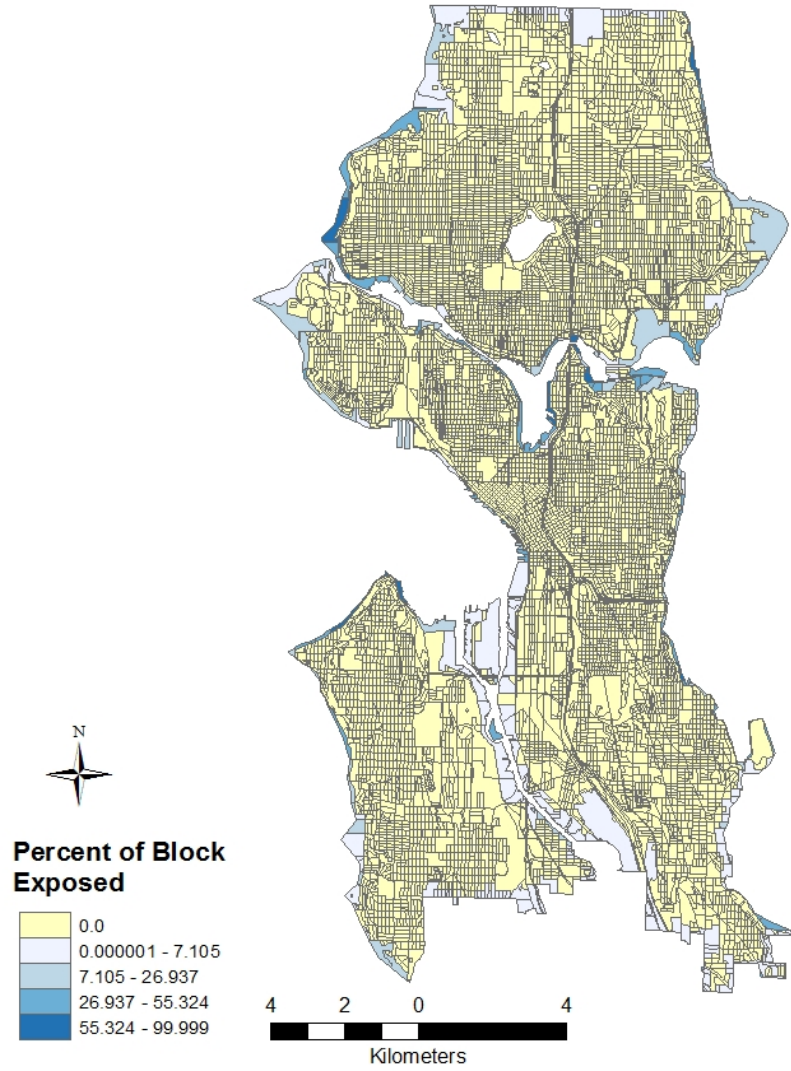
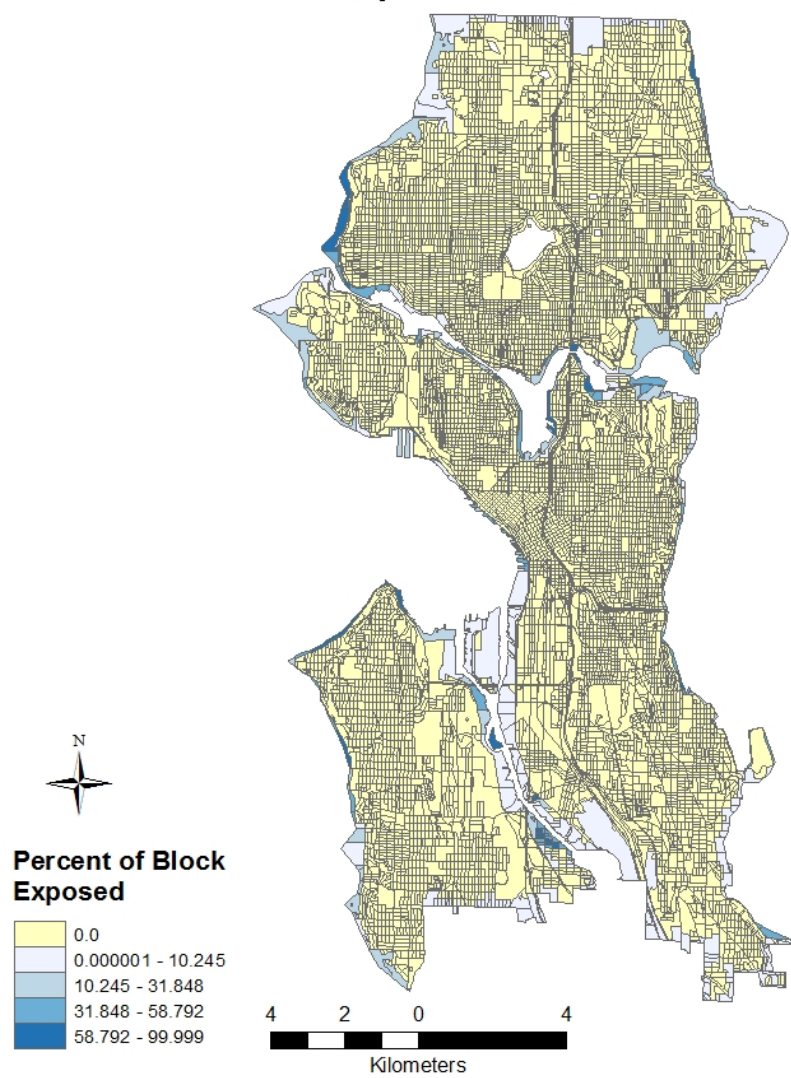


Figure 4: 0.105 Exposure Map

**Scenario: 3.804 (m)  
Exposure**



**Figure 5: 3.804 Exposure Map**

### Scenario: 4.610 (m) Exposure

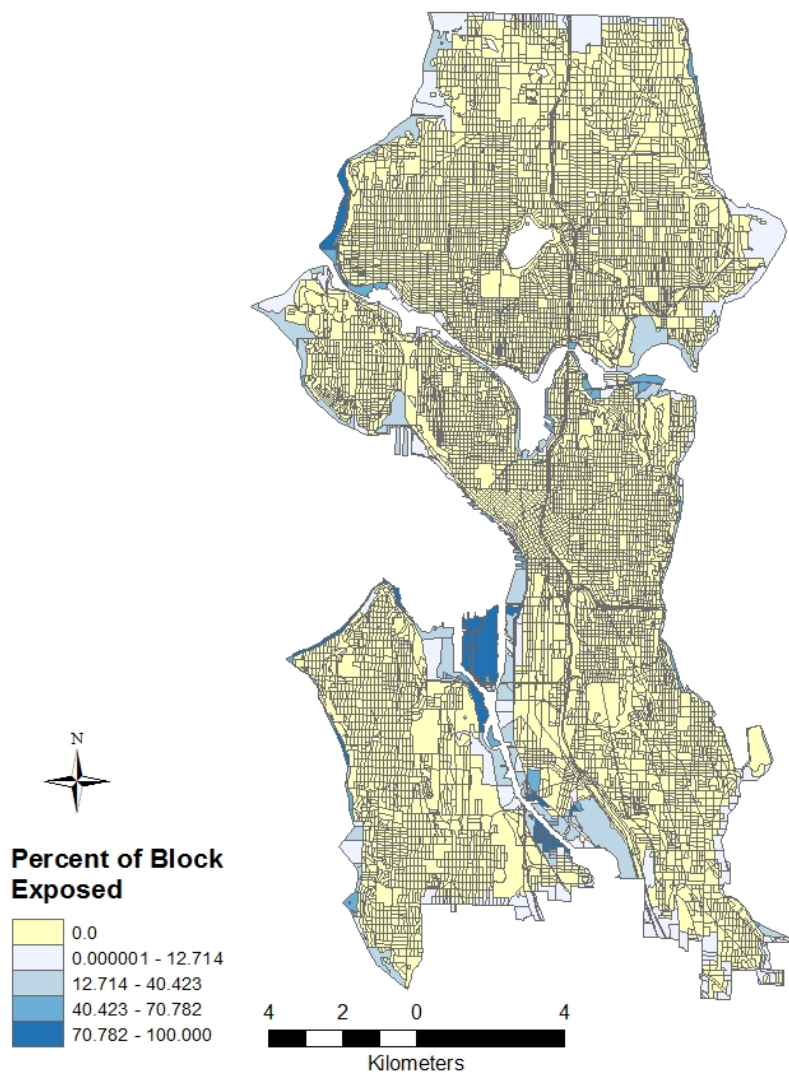


**Figure 6: 4.610 Exposure map**

The maps indicate that high tide will affect the census blocks located along waterways more than the coastal blocks. For example, the island located on the lower half of the Seattle, increases in exposure from 0.00001 % to over 70 % over the four scenarios. The blocks along the lower waterway are .00001 % exposed to over 40 % exposed. The blocks along

the upper waterway change very little. This indicates that there will be little change in exposure due to SLR and because of the vulnerability will change very little.

### 3.2: SERV

Results for the adaptive capacity and sensitivity scores for the SERV model were calculated using a PCA with the variables from tables 2 and 3, respectively. Negative component loadings indicate variables that are not present, but are still significant within the block. Chosen components for both adaptive capacity and sensitivity had eigenvalues greater than 1.0 and the retained variables had loading scores with absolute values of greater than 0.45. The discarded variables and components did not meet these criteria. The four adaptive capacity components explain 59.598% of the variance and include 13 of the original 14 variables. The percent of the Seattle's employees located in each block was not one of the components. The components are displayed in Table 5. For both adaptive capacity and sensitivity, the scores were calculated as a linear combination of the loading factors and percent variance explained for the factors and principle components that met the stated criteria.

<b>Adaptive Capacity: PCA Results</b>				
<b>Component</b>	<b>Eigenvalue</b>	<b>% Variance Explained</b>	<b>Variables</b>	<b>Component Loading</b>
1. Income, Education, and Ethnicity	3.44	23.406	Not_White	0.646
			Pct_Below_Pov	0.722
			Not_HSGrad	0.904
			College_Grad	-0.857
			Pct_Unemployed	0.622
2. Household structure and ownership, Age, and Race	2.541	17.809	Under5	0.624
			Above_65	0.627
			F_HeadHoushold	0.498
			White	0.701
			Owner_Occupied	0.842
3. Economic Base	1.26	8.95	Pct_TaxParVal	0.485
			Pct_Bus_Revenue	0.679
4. Equality	1.103	9.433	Gini_Index	0.822
Total Variance Explained:		59.598		

**Table 5: Adaptive Capacity: PCA Results**

The adaptive capacity results provide four principle components. The first includes income, education, and ethnicity, and explains 23.406 % of variance. The second component explains 17.809 % of the variance and includes household structure and ownership along with residents' age and race. The third component includes economic base data and explains 8.950%. The fourth and final component includes equality information and explains 9.433% of the variance. The map in Figure 7 shows the adaptive capacity results in units of standard deviation.

## SERV: Adaptive Capacity Results

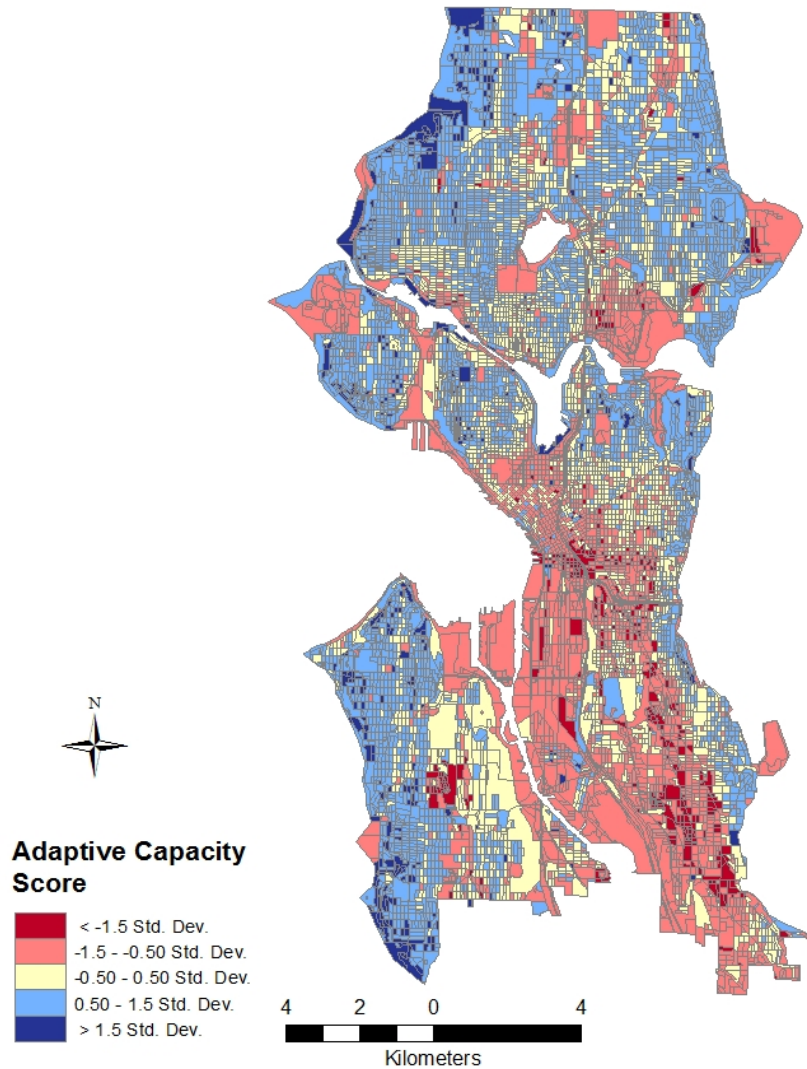


**Figure 7: SERV: Adaptive Capacity Result map**

Figure 7 shows areas with higher adaptive capacity scores in dark blue and areas with lower adaptive capacity in dark red. Areas with average adaptive capacity are in yellow. In many cases, the blocks along the waterways have the lowest or average adaptive capacity. These blocks are also more exposed to SLR, decreasing their vulnerability. In this

case, the coastal blocks, specifically those on the west side of the city have the highest adaptive capacity, indicating that they are better able to recover from any SLR. There are few blocks with average adaptive capacity and the low levels of adaptive capacity are located in the southern half of the city. The four sensitivity principle components explain 69.523% of the variance and include 11 of the original 12 variables. The percent of residents under 5 in each block was not one of the components. The components are displayed in Table 6.

<b>Sensitivity: PCA Results</b>				
<b>Component</b>	<b>Eigenvalue</b>	<b>% Variance Explained</b>	<b>Variables</b>	<b>Component Loading</b>
1. Age, Sex, and Race	4.12	21.892	F_Pop Above_65 Med_age White	0.834 0.672 0.918 0.887
2. Population and home ownership	1.94	18.423	Pct_Pop Total_Households Renter_occupied	0.884 0.916 0.689
3. Economic Base	1.493	13.95	Pct_Employees Bus_Revenue	-0.909 -0.903
4. Household Structure and Ethnicity	1.348	15.258	F_HeadHoushold Not_White	0.82 0.842
Total Variance Explained: 69.523				

**Table 6: Sensitivity: PCA Results**

The sensitivity results show four principle components. The first includes age, sex, and race, and explains 21.892 % of variance. The second component explains 18.423 % of the variance and includes population and home ownership data. The third component includes economic base data and explains 13.95 % of the variance. The fourth and final component includes household structure and ethnicity information and explains 13.95 % of the variance. The map in Figure 8 shows the sensitivity results in units of standard deviation. Higher sensitivity is indicated in red and dark red and lower sensitivity is indicated in blue. Blocks along the waterways are less sensitive to SLR, however they are also more exposed and have less adaptive capacity. This indicates that although, these blocks are not as affected by SLR, they will have a harder time recovering from any inundation they may experience. In many cases, the areas with higher sensitivity are also the areas with lower adaptive capacity. This indicates that if exposed to a hazard, these areas will have a harder time recovering from the disaster because they have fewer resources before and after the event to aid them. Although the blocks in the southeastern quadrant of the city have limited exposure, they have higher levels of sensitivity as well as lower levels of adaptive capacity, indicating that they will have high levels of vulnerability.

## SERV: Sensitivity Results

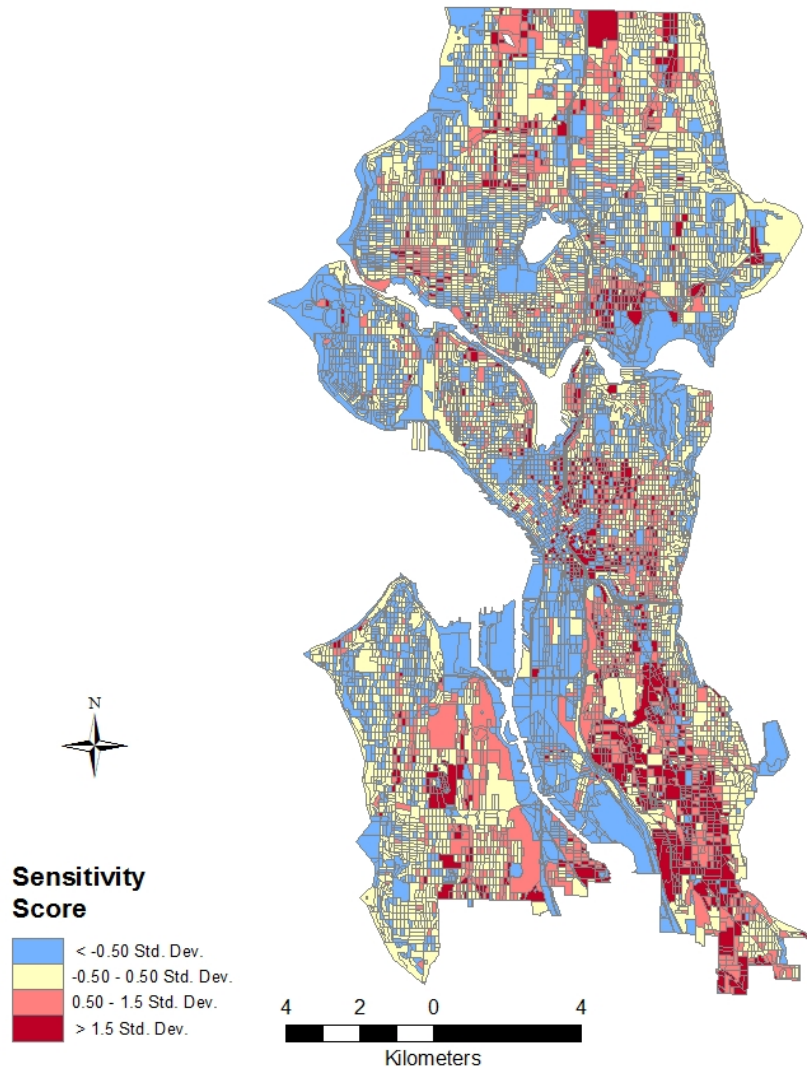


**Figure 8: SERV: Sensitivity Results map**

Figure 8 shows areas with higher sensitivity scores in dark red and areas with lower sensitivity in blue. Areas with average sensitivity are in yellow. Figures 9, 10, 11, and 12 show the SERV score for Seattle with 0.010 m, 0.105 m, 3.804 m and 4.610 m of SLR.

**SLR Scenario: 0.010 (m)**  
**SERV**

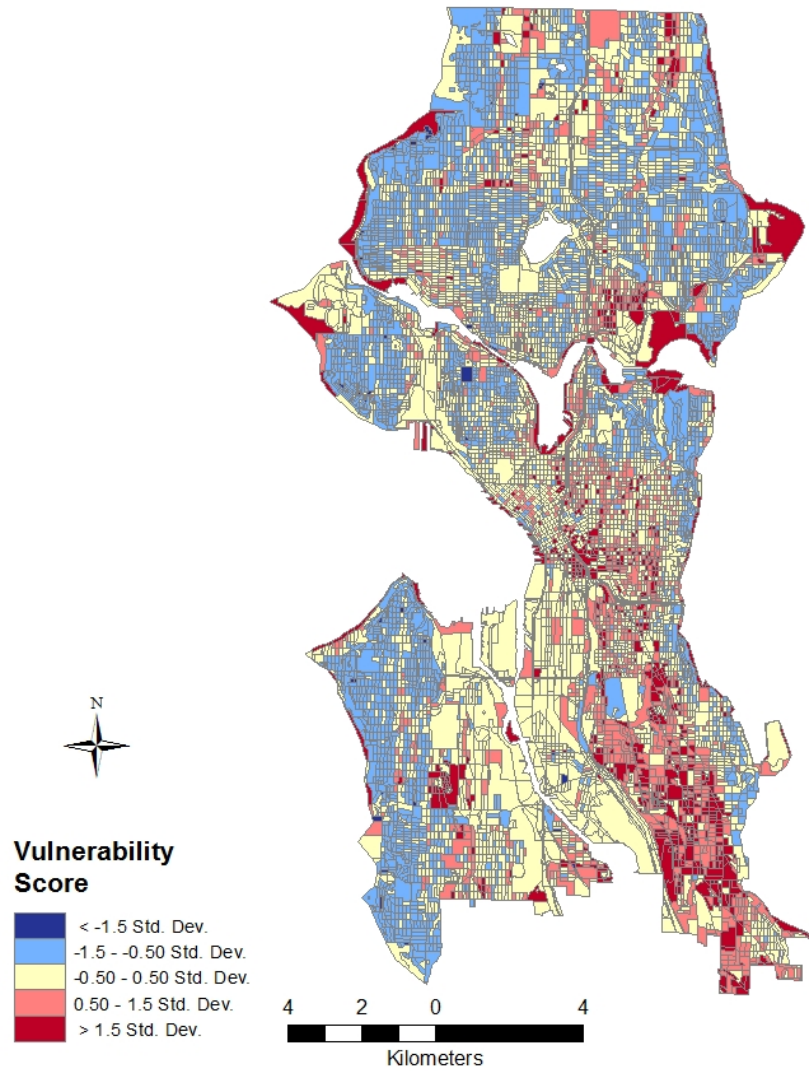


**Figure 9: SERV: 0.010 map**

**SLR Scenario: 0.105 (m)**  
**SERV**

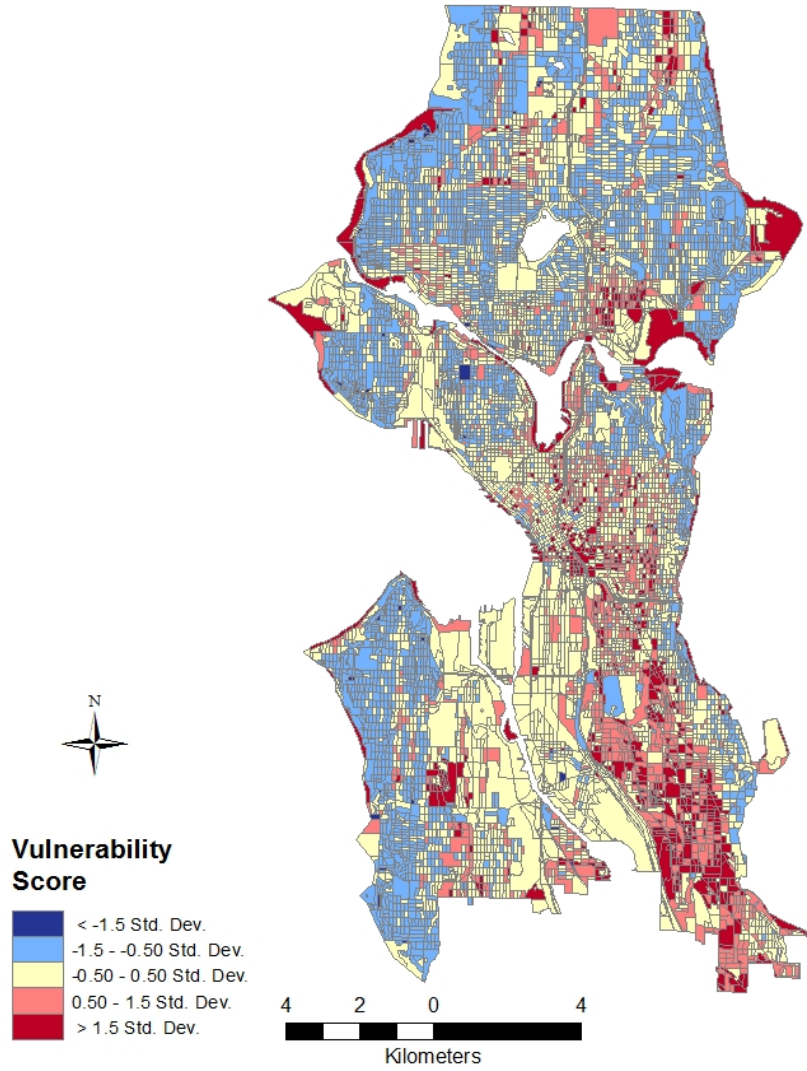


**Figure 10: SERV: 0.105 map**

**SLR Scenario: 3.804 (m)**  
**SERV**

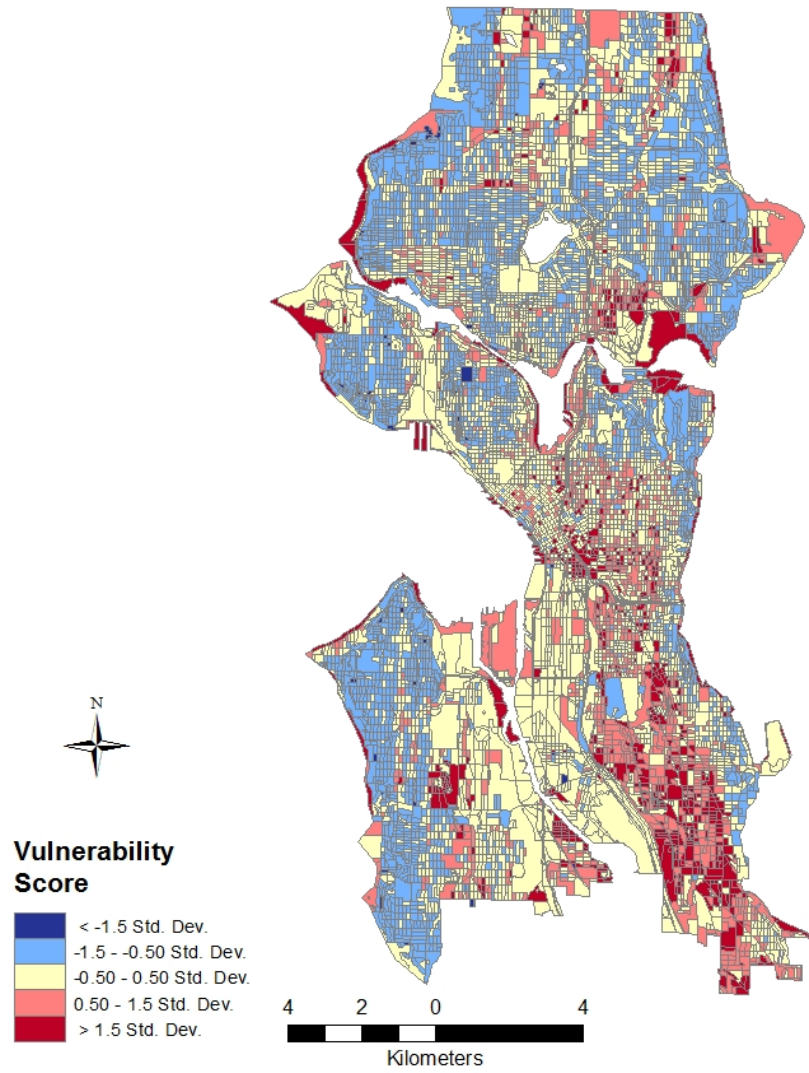


**Figure 11: SERV: 3.804 map**

**SLR Scenario: 4.610 (m)  
SERV**

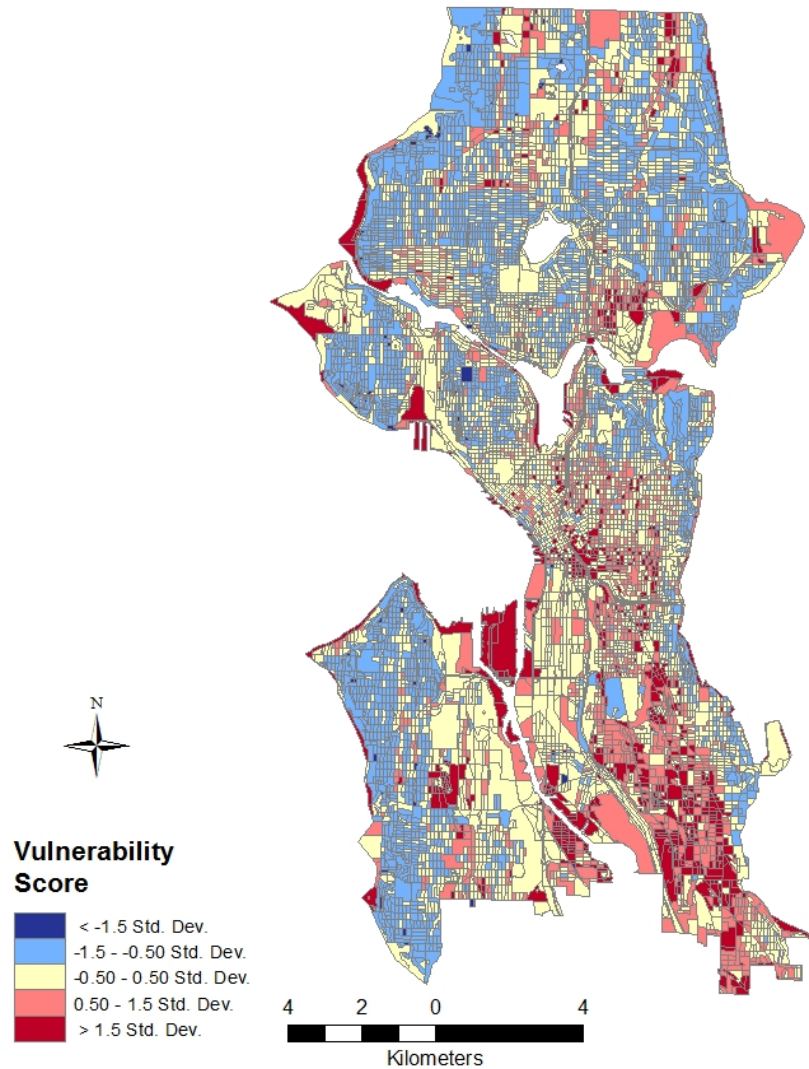


**Figure 12: SERV: 4.610 map**

Areas of dark blue indicate lower vulnerability, whereas areas of dark red indicate higher levels of vulnerability. Higher vulnerability areas are focused in the southeastern quadrant of the city. The vulnerability along the lower waterway increases as the exposure to SLR increases. The areas with lower vulnerability are in the southwestern, northwestern and

northeastern quadrants of the city. The center of the city generally has average levels of vulnerability. Areas with average or above average sensitivity scores and lower and below average adaptive capacity scores are the areas that are most vulnerable. However, the areas with high levels of exposure are also more vulnerable regardless of the adaptive capacity and vulnerability scores.

### 3.3: GWSERV

Sensitivity and adaptive capacity components for the GWSERV model are calculated using a GWPCA. The GWSERV results differ from the SERV results because in the GWSERV results, all components include only one variable, as opposed to several in the SERV model. As with the SERV model, the first four components were chosen for the adaptive capacity and sensitivity indices. The first four adaptive capacity components explain between 93.60% and 100.00% of the variance in each census block. Figure 13 displays the total variance explained by the four components in each block. For all the percent variance explained maps, lighter yellow values are lower explained variance and darker red are higher values. The areas of lower total explained variance are often at the center the landmasses indicating that the higher number of surrounding blocks, the less variance can be explained by the components. This indicates that the more information that is available from external blocks, the less one can determine causes of variability.

### Adaptive Capacity: Total Percent Variance Explained

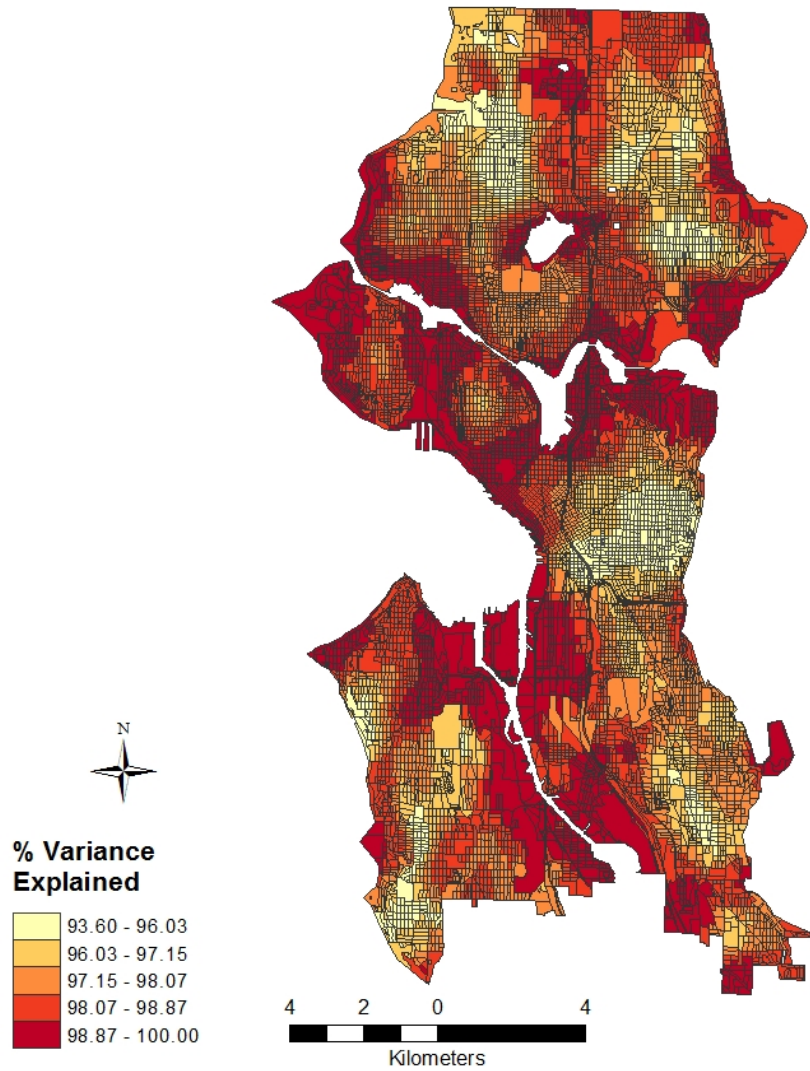


**Figure 13: GWSERV: Adaptive Capacity Total PVE map**

The first adaptive capacity components are displayed in Figure 14.

### Adaptive Capacity: Component 1

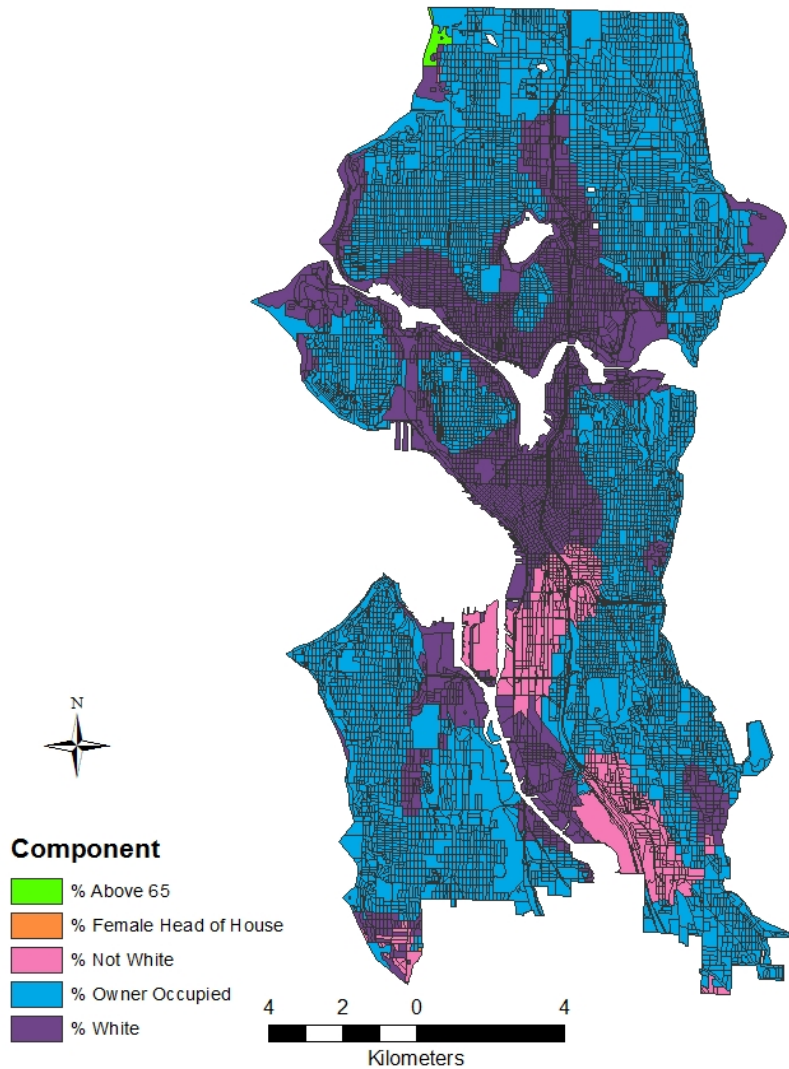


**Figure 14: GWSERV: Adaptive Capacity Component 1 map**

The most prevalent component is the percent of owner occupied homes (blue) then the percent of white residents (purple). This indicates that, in most areas, the component that is most important to the adaptive capacity of the census block is the percent of owner occupied homes. Owner occupied homes have more agency and are of a higher economic

status than renter occupied homes because they are more likely to take steps to improve their homes to mitigate the effects of hazards. Historically, white populations have more agency and are better able to access recourses that improve their adaptive capacity. The remaining blocks had the percent of not white residents (pink), the percent of elderly residents (green), and the percent of female heads of household as the first component (Morrow, 1999). The explained variance for adaptive capacity's first component is displayed in Figure 15. The first component explains between 58.41 % and 99.89 % of the variance in each block. The trend of the percent variance explained indicates that the more variance the first component explains in a block compared to the neighboring blocks, the less the second, third, and fourth variables will explain.

### Adaptive Capacity Component 1: Percent Variance Explained

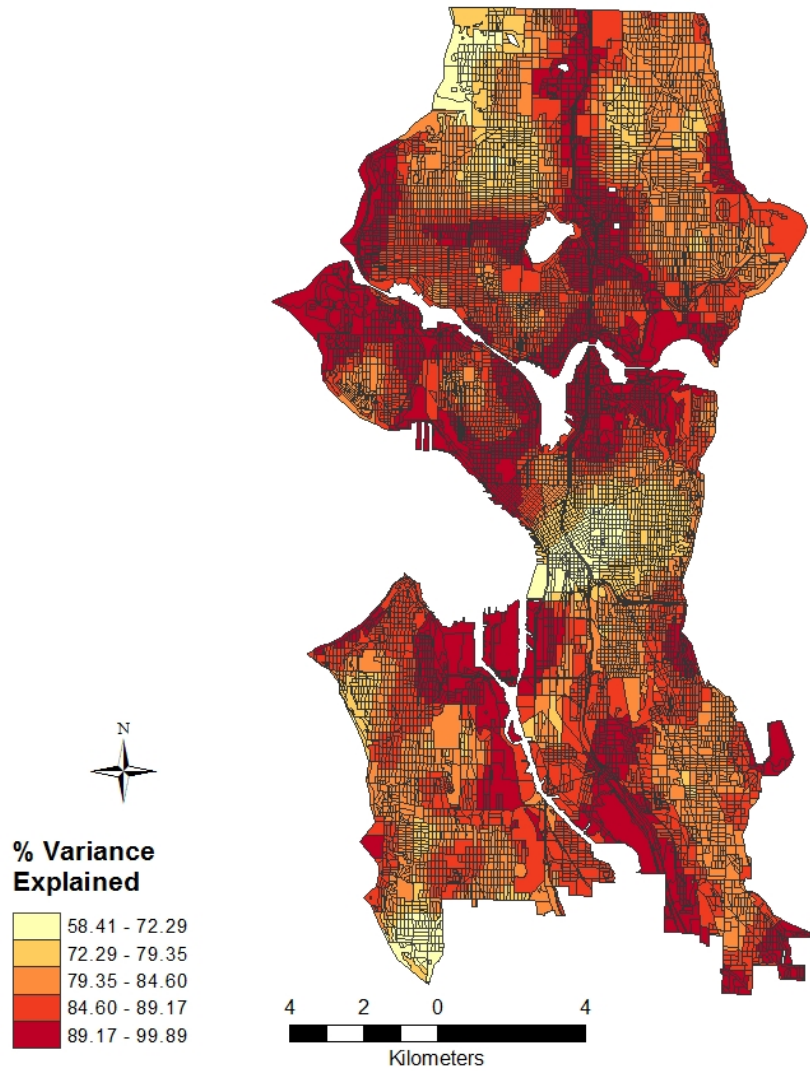


**Figure 15: GWSERV: Adaptive capacity Component 1 PVE map**

The second adaptive capacity component is displayed in Figure 16.

## Adaptive Capacity: Component 2

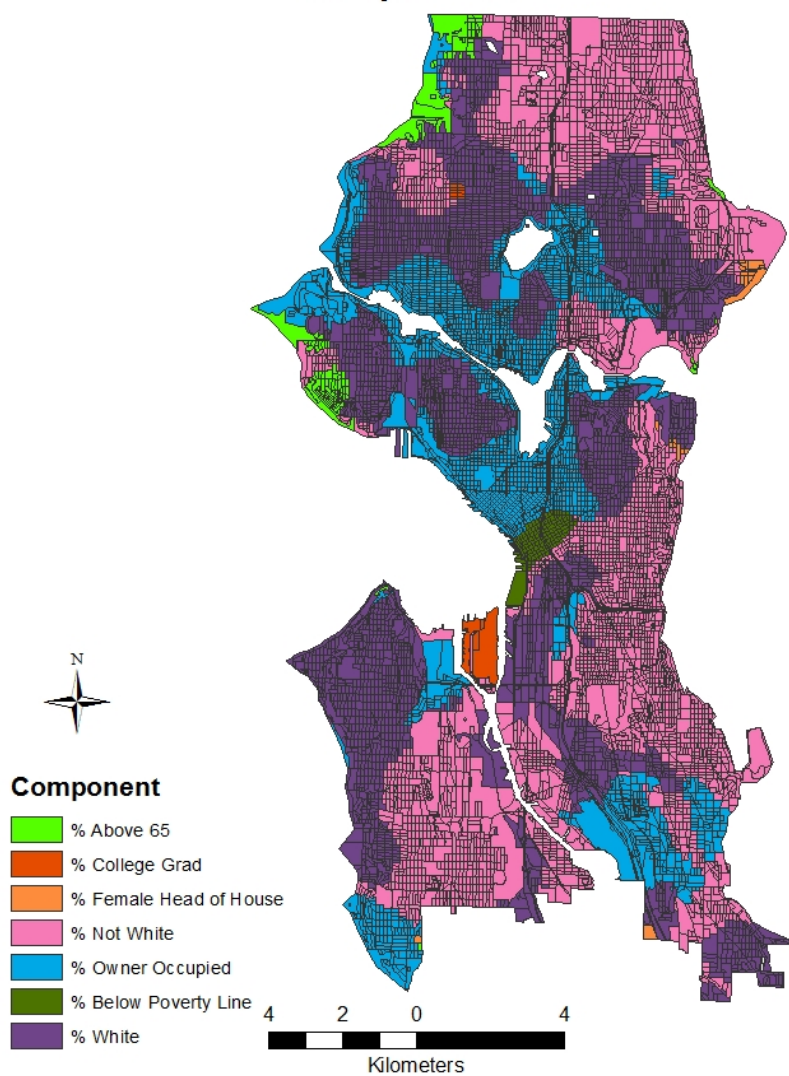


**Figure 16: GWSERV: Adaptive Capacity Component 2 map**

The second component that is most likely to be present is the percent of not white residents in the block. In addition to the first component, the census blocks could also have a second of the percent of college graduates (red) and the percent of residents that are under the poverty line (dark green). The explained variance for adaptive capacity's second component

is displayed in Figure 17. The second component explains between 0.10 % and 22.23 % of the variance in each block.

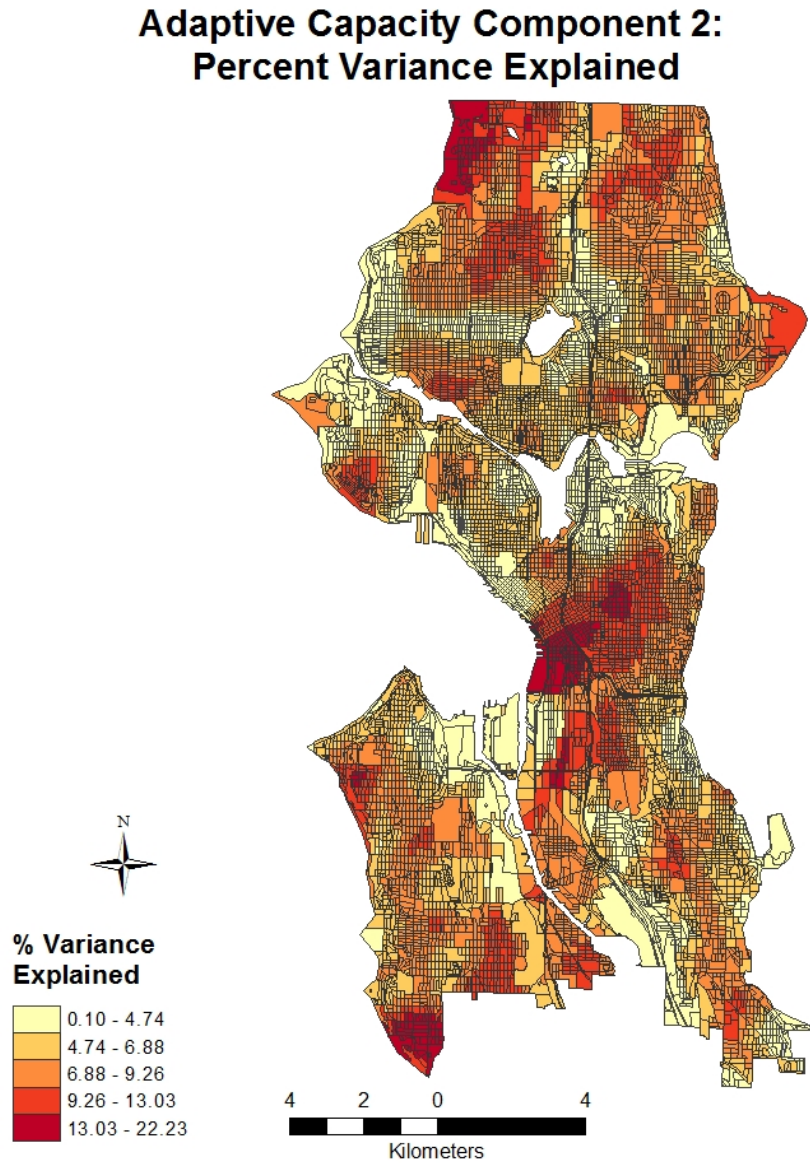


**Figure 17: GWSERV: Adaptive Capacity Component 2 PVE map.**

The third adaptive capacity component is displayed in Figure 18.

### Adaptive Capacity: Component 3

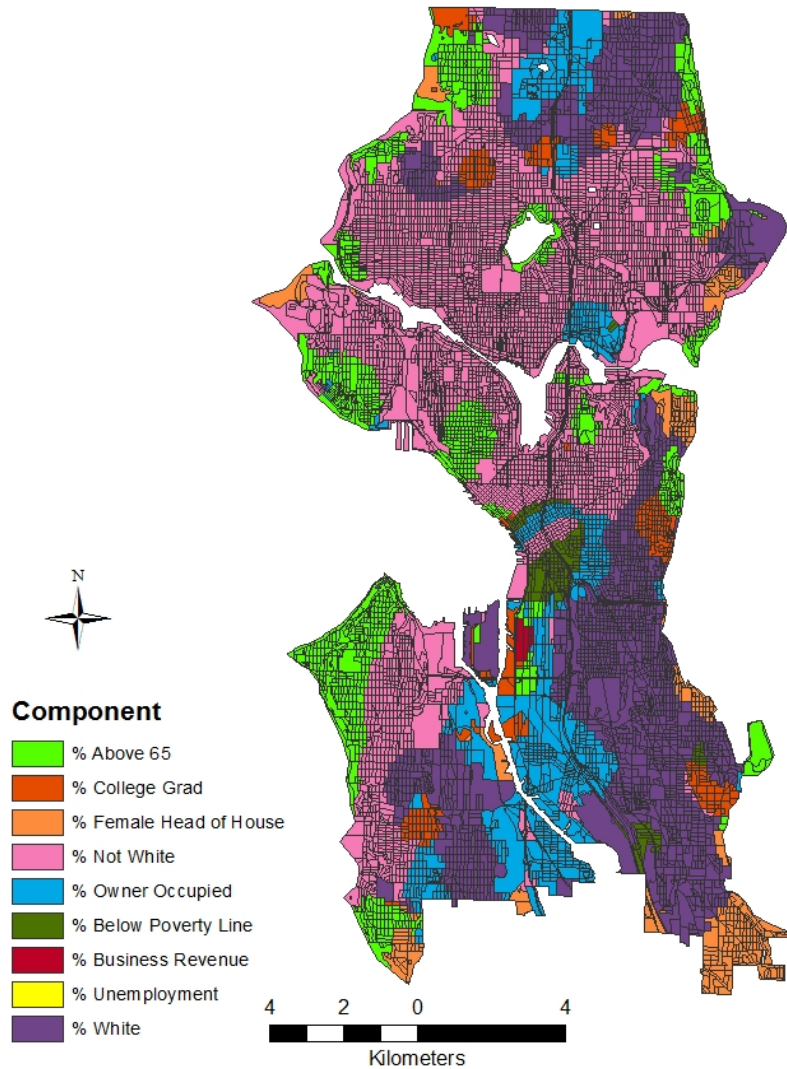


**Figure 18: GWSERV: Adaptive Capacity Component 3 map**

The distribution of the third component is more varied than the first two. For example, the blocks where the percent of college graduates and the percent of female heads of household are not always clustered. However, the blocks that have the percent of not white residents as the third component are clustered. The explained variance for adaptive capacity's third

component is displayed in Figure 19. The third component explains between 0.005 % and 14.43 % of the variance in each block.

### Adaptive Capacity Component 3: Percent Variance Explained

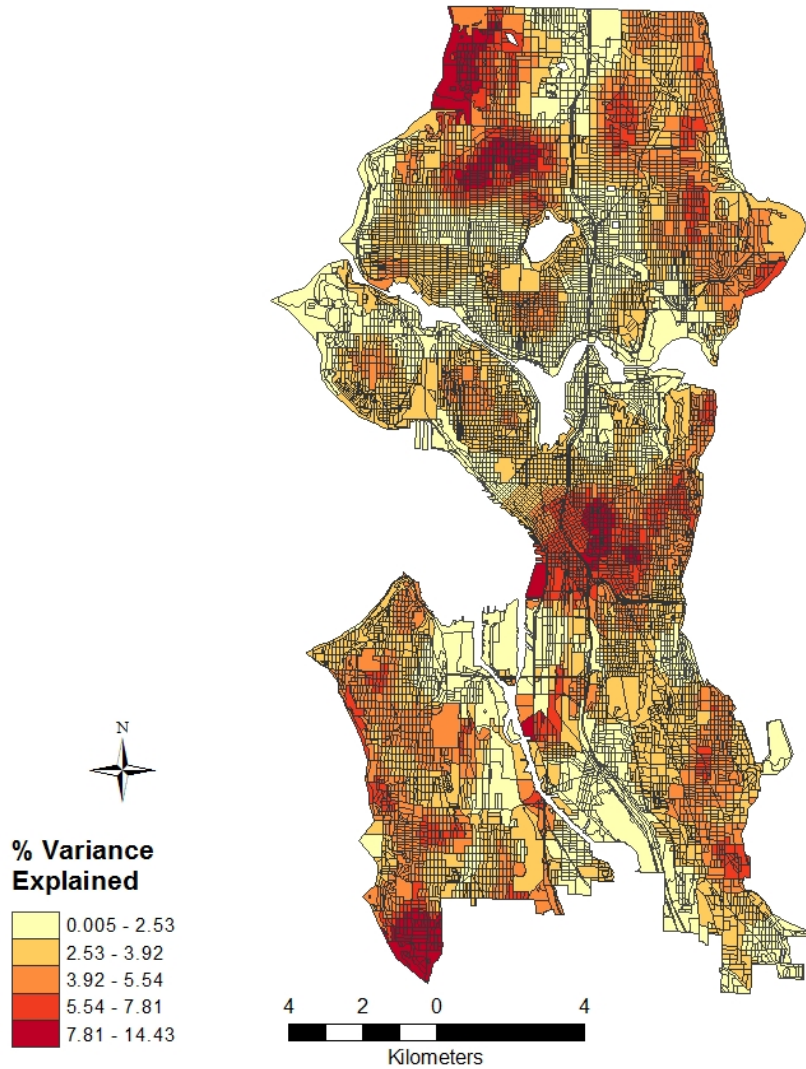


**Figure 19: GWSERV: Adaptive Capacity Component 3 PVE map**

The fourth adaptive capacity component is displayed in Figure 20.

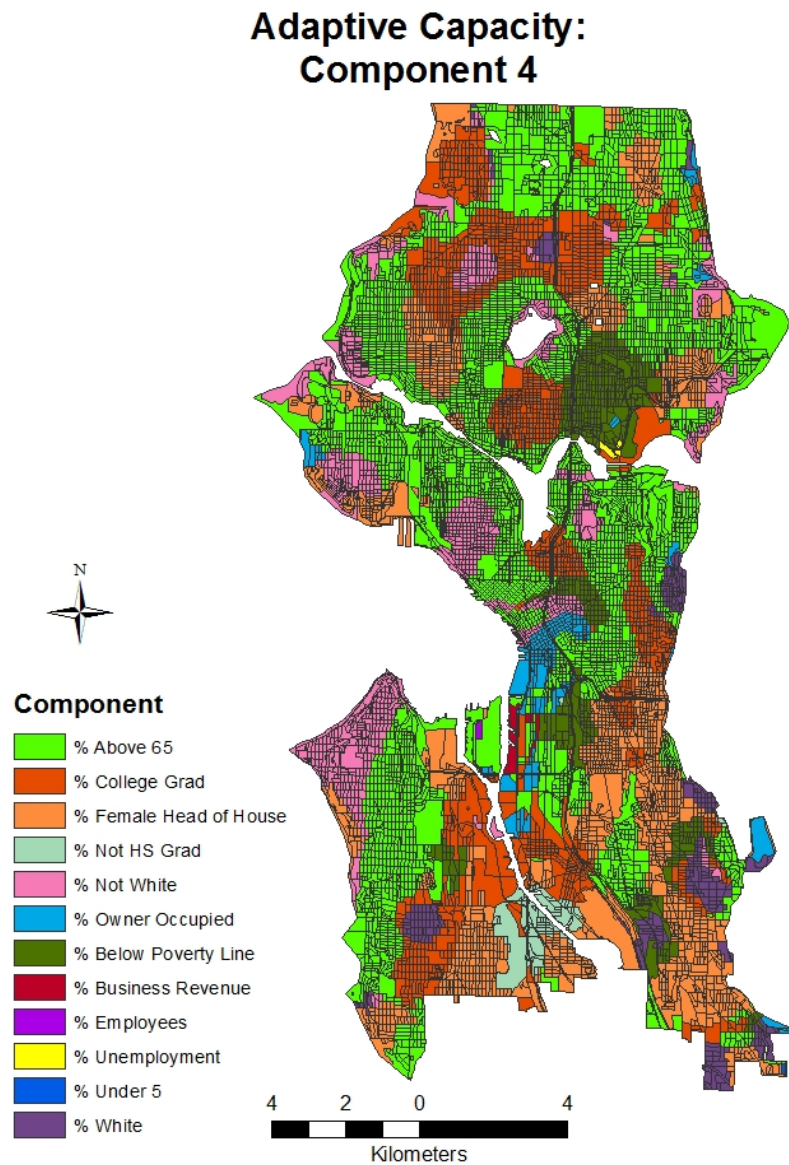


**Figure 20: GWERV: Adaptive Capacity Component 4 map**

The final principle component shows the most variability between the blocks. In this case the blocks could have 12 different components, including the percent of unemployed residents and the percent of residents that are under 5. The explained variance for adaptive

capacity's fourth component is displayed in Figure 21. The fourth component explains between 0.002 % and 8.66 % of the variance in each block.

### Adaptive Capacity Component 4: Percent Variance Explained

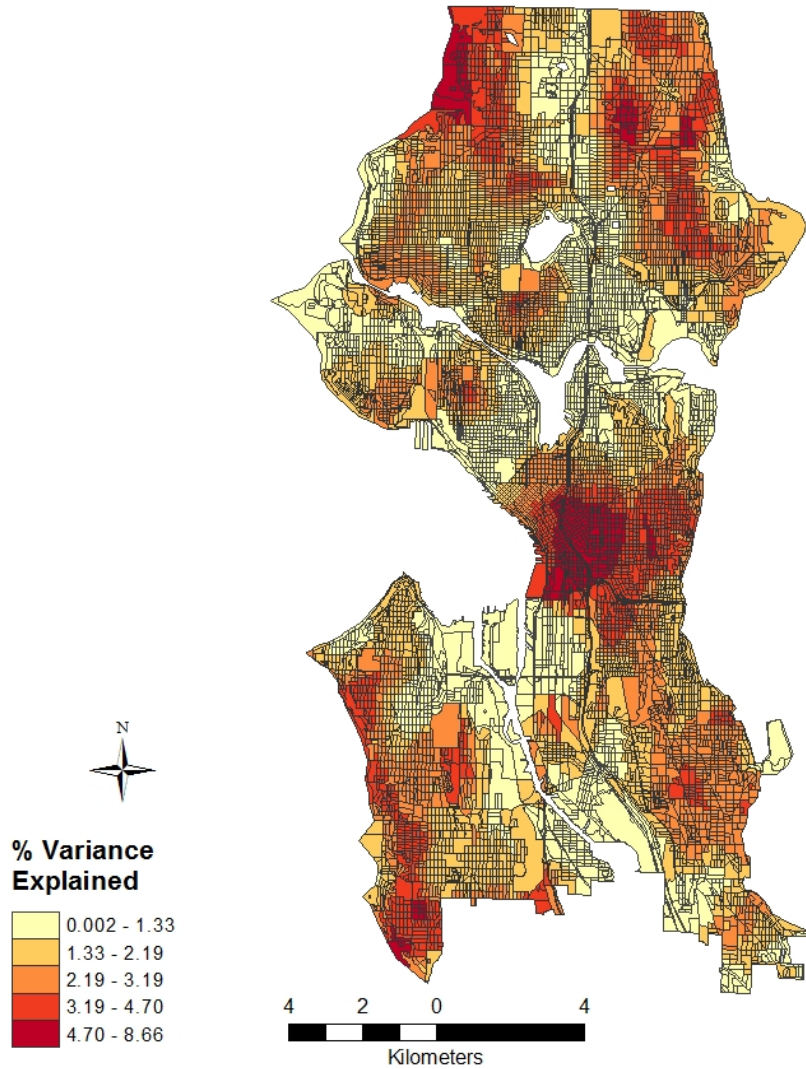


**Figure 21: GWSERV: Adaptive Capacity Component 4 PVE map**

Figure 22 shows the deviation of the calculated adaptive capacity scores from the mean. Blue represents higher levels of adaptive capacity and dark red represents lower

levels of adaptive capacity. The results indicate that, in general, the blocks located along waterways have the least adaptive capacity. This indicates that if exposed to a hazard, they will have a harder time recovering from the event. These areas are also the most exposed, further indicating that they will have lower vulnerability.

### **GWSERV: Adaptive Capacity Results**

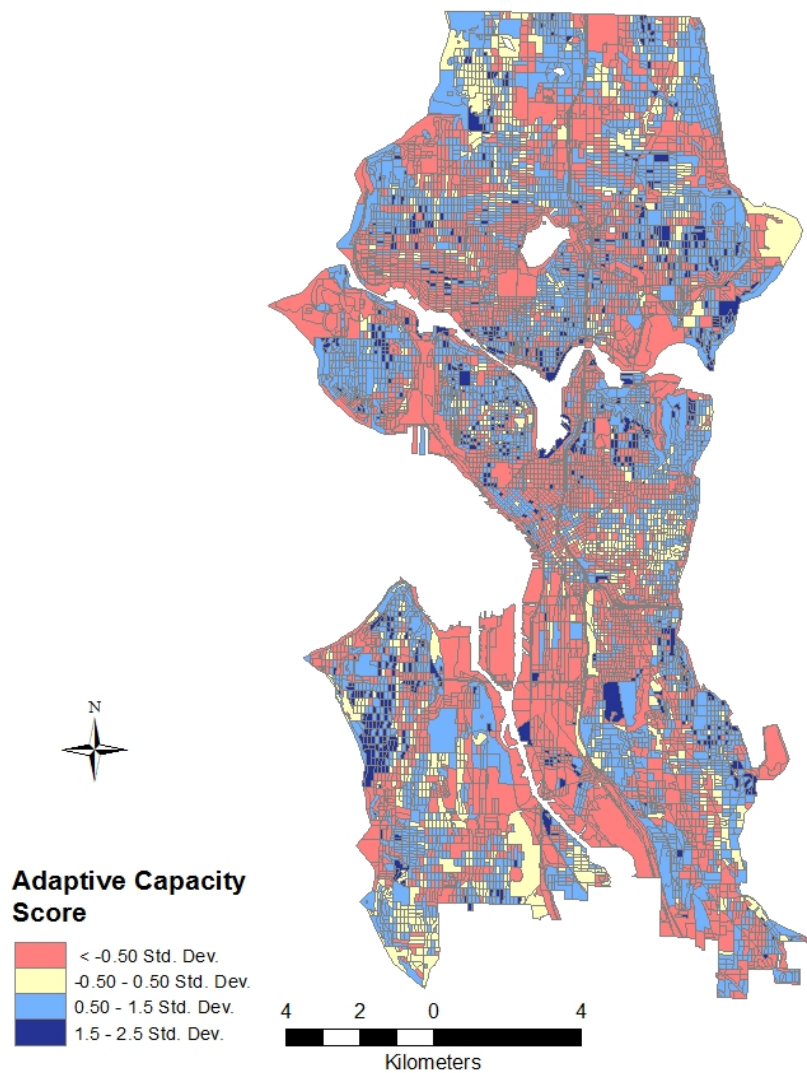


**Figure 22: GWSERV: Adaptive Capacity Results map**

The first four sensitivity components explain between 92.36% and 100.00% of the variance in each block. Figure 23 displays the total variance explained per block. As with adaptive capacity, the higher levels of explained variance are concentrated along the edges of the landmasses, indicating that the more information available, the less variance that can be explained. As with adaptive capacity, the more variance explained by the first component, the less variance subsequent components will explain.

**Sensitivity:  
Total Percent Variance Explained**

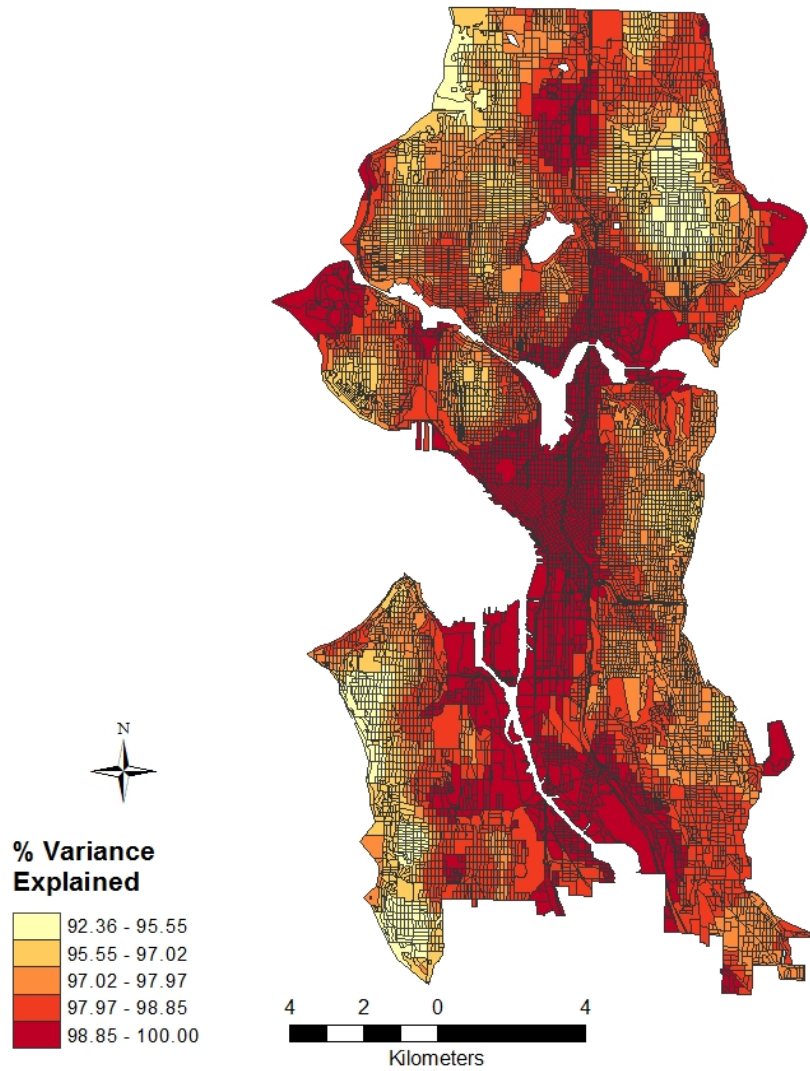


**Figure 23: GWSERV: Sensitivity Total PVE map**

The first sensitivity component is displayed in Figure 24.

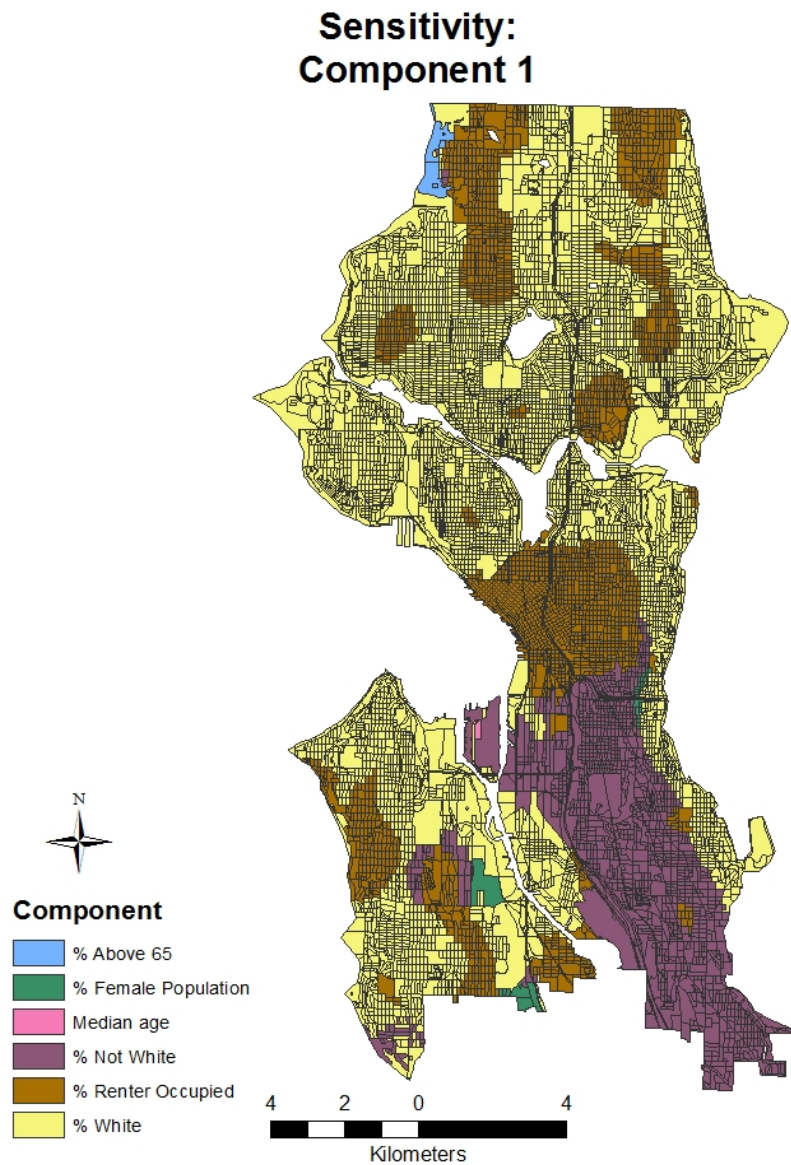


**Figure 24: GWSERV: Sensitivity Component 1 map**

The most prevalent indicator for sensitivity is the percent of the white population in the census block then the percent of not white residents and renter occupied homes. Both renter occupied homes and not white populations are historically more sensitive to disasters because they lack access to resources (Morrow, 1999). The explained variance for

sensitivity's first component is displayed in Figure 25. The first component explains between 56.89 % and 99.9 % of the variance in each block.

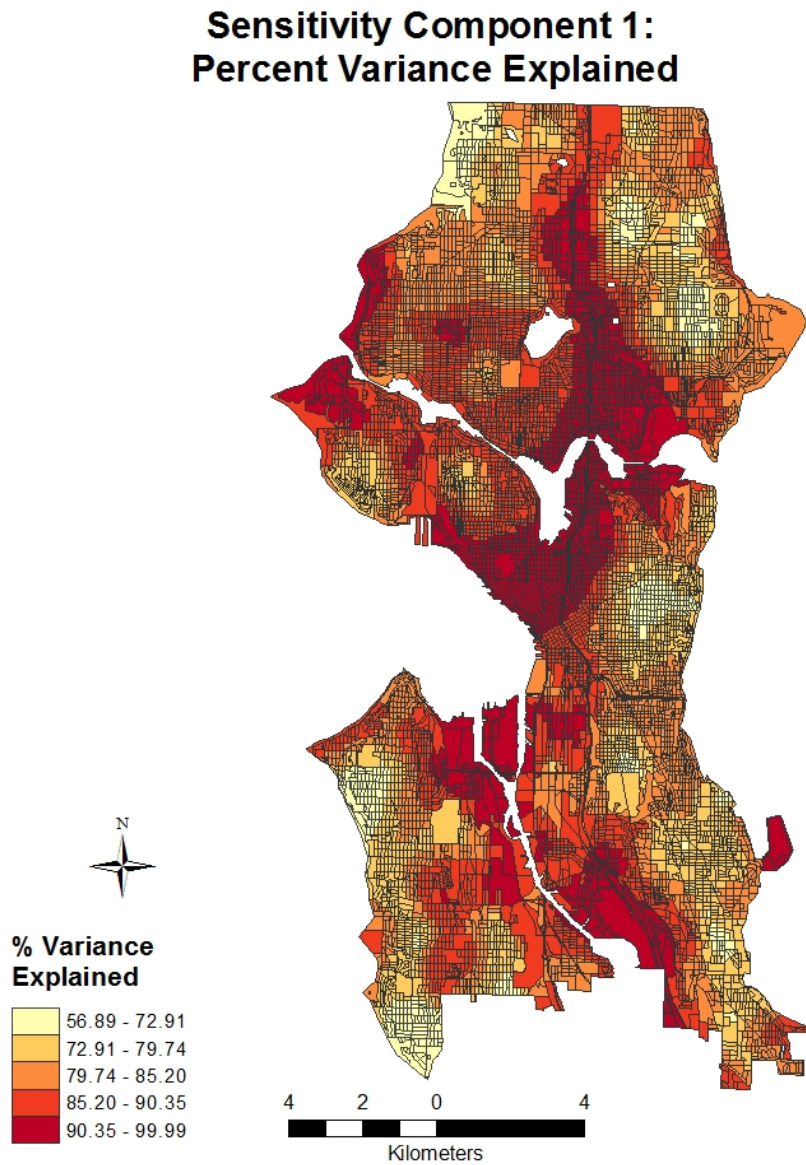


**Figure 25: GWSERV: Sensitivity Component 1 PVE map**

The second sensitivity component is displayed in Figure 26.

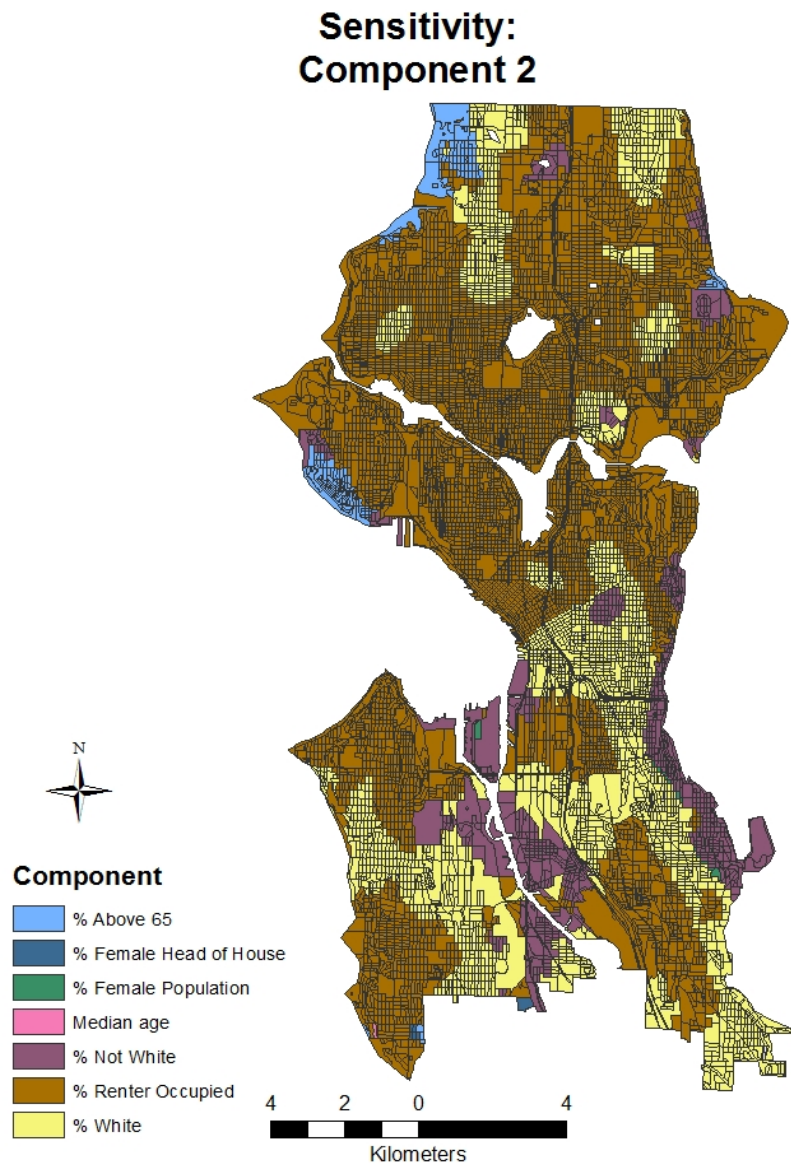


**Figure 26: GWSERV: Sensitivity Component 2 map**

The most prevalent second component is the percent of renter occupied buildings (brown) then the white population (yellow). The explained variance for sensitivity's second component is displayed in Figure 27. The second component explains between 0.01 % and 23.78 % of the variance in each block.

## Sensitivity Component 2: Percent Variance Explained

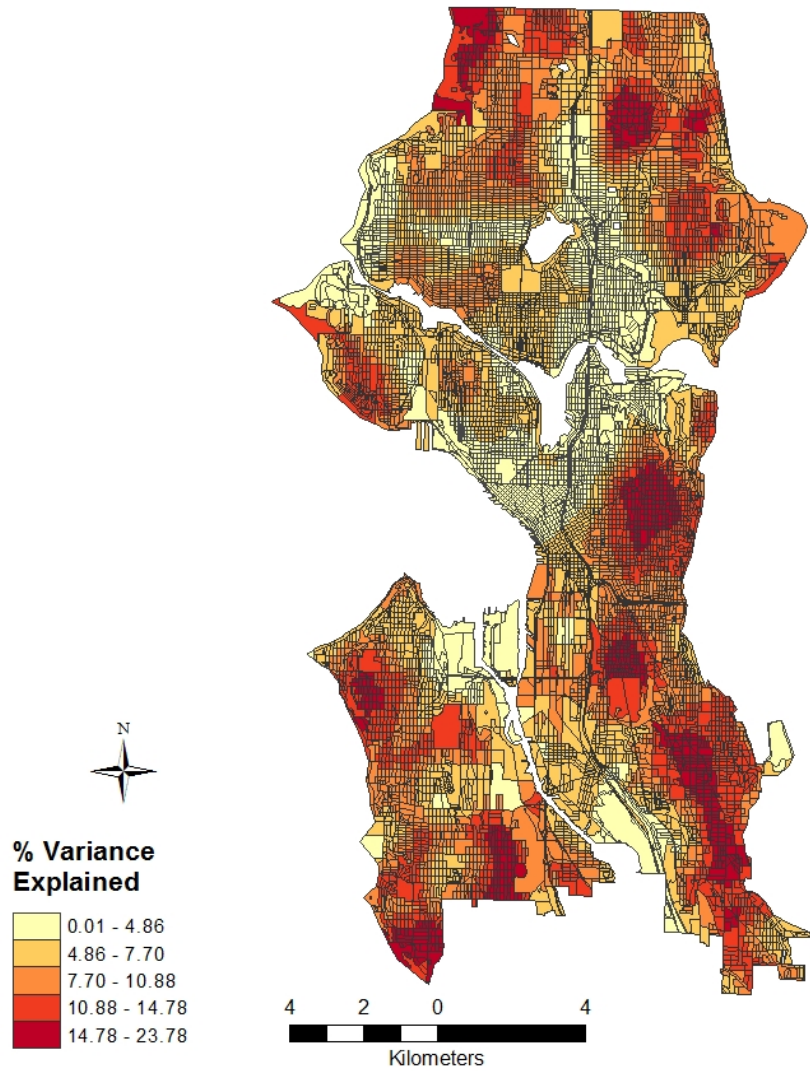


**Figure 27: GWSERV: Sensitivity Component 2 PVE map**

The third sensitivity component is displayed in Figure 28.

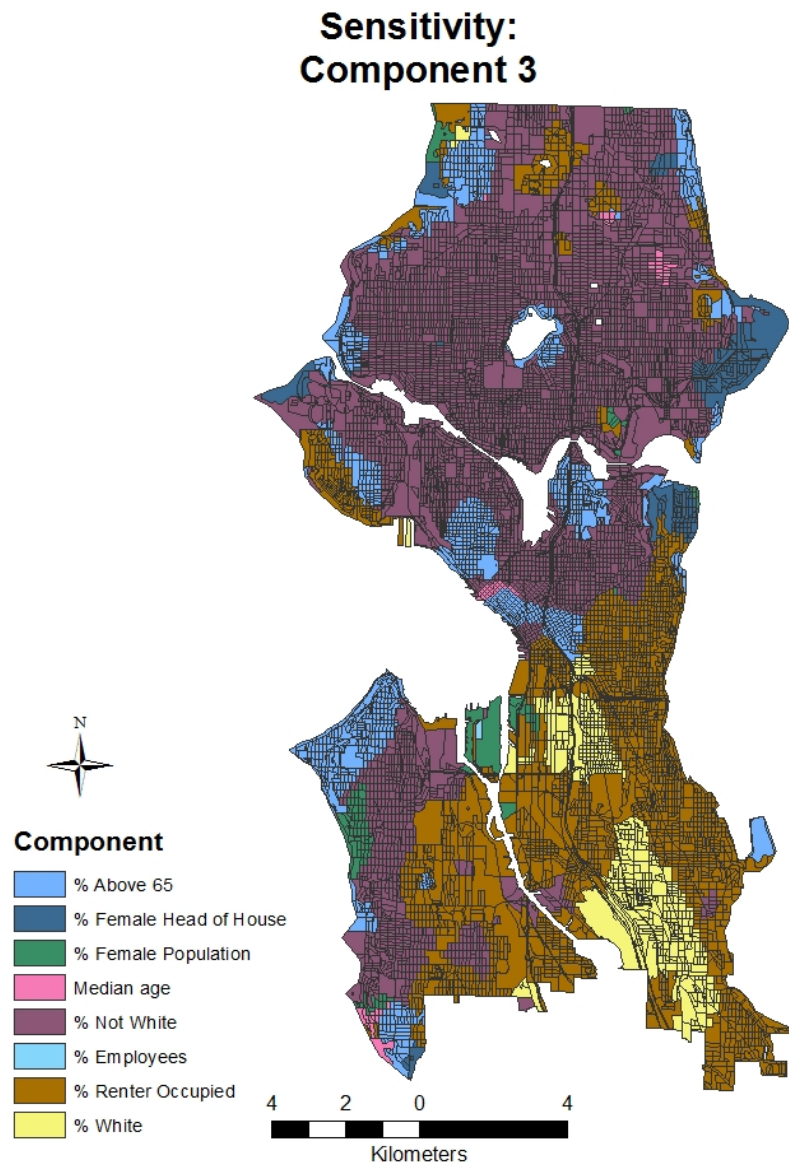


**Figure 28: GWSERV: Sensitivity Component 3 map**

The percent not white population (purple) is the most prevalent third principle component followed by the percent of renter occupied buildings (brown). The explained variance for sensitivity's third component is displayed in Figure 29. The third component explains between 0.000017 % and 14.55 % of the variance in each block.

### Sensitivity Component 3: Percent Variance Explained

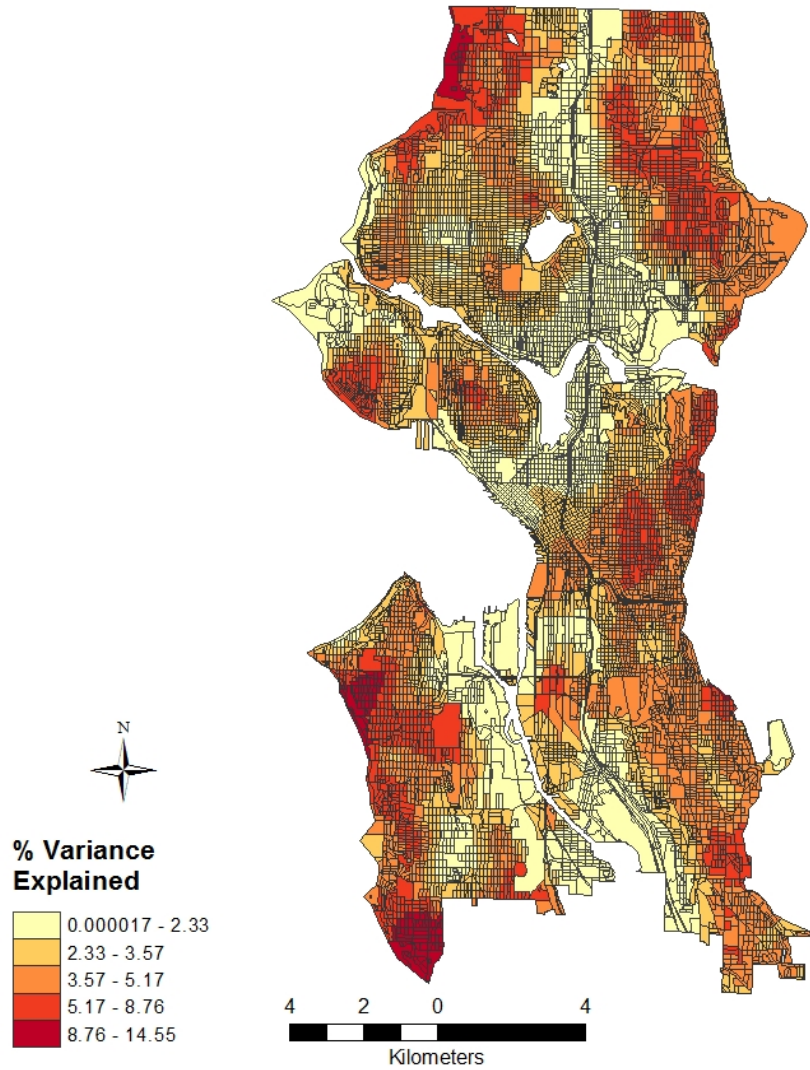


**Figure 29: GWSERV: Sensitivity Component 3 PVE map**

The fourth sensitivity component is displayed in Figure 30.

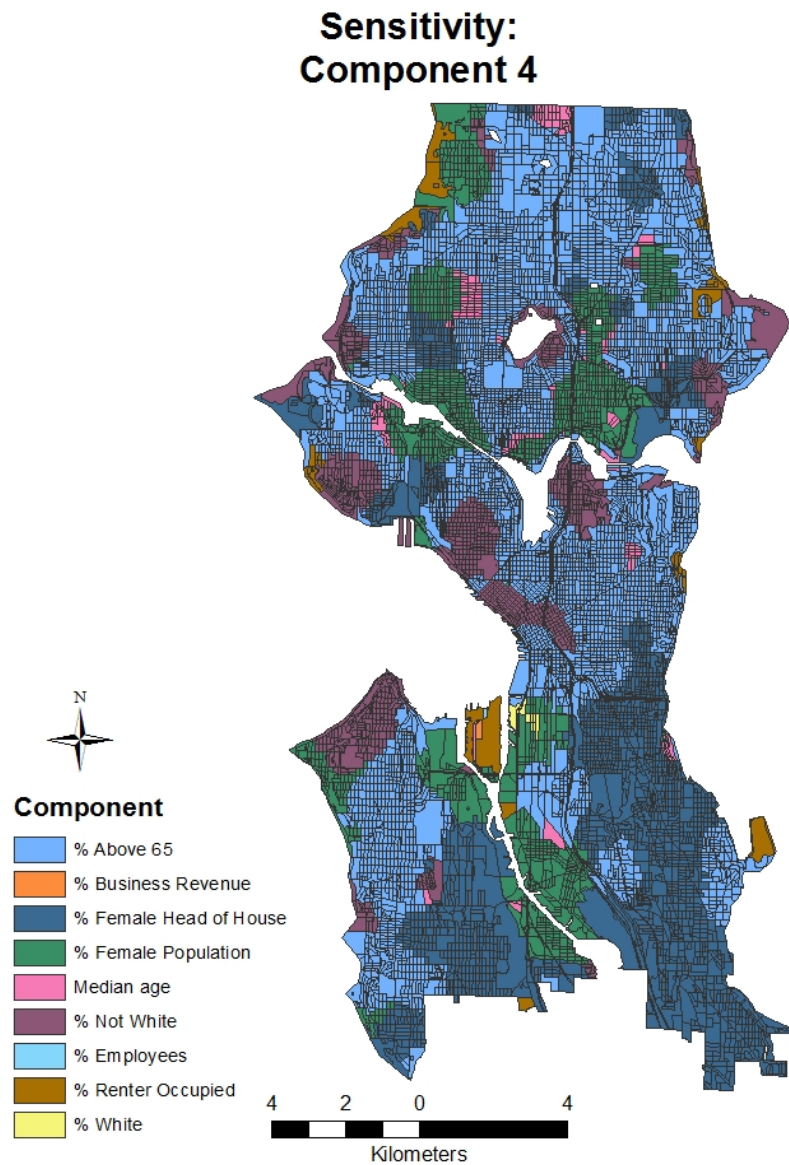


**Figure 30: GWSERV: Sensitivity Component 4 map**

The percent of the population above 65 and the percent of female heads of households (dark blue) are the most prevalent fourth components. Unlike in the adaptive capacity results, the sensitivity components remain generally clustered, indicating that there is a block effect.

The explained variance for sensitivity's first component is displayed in Figure 31. The fourth component explains between 0.00 % and 9.00 % of the variance in each block.

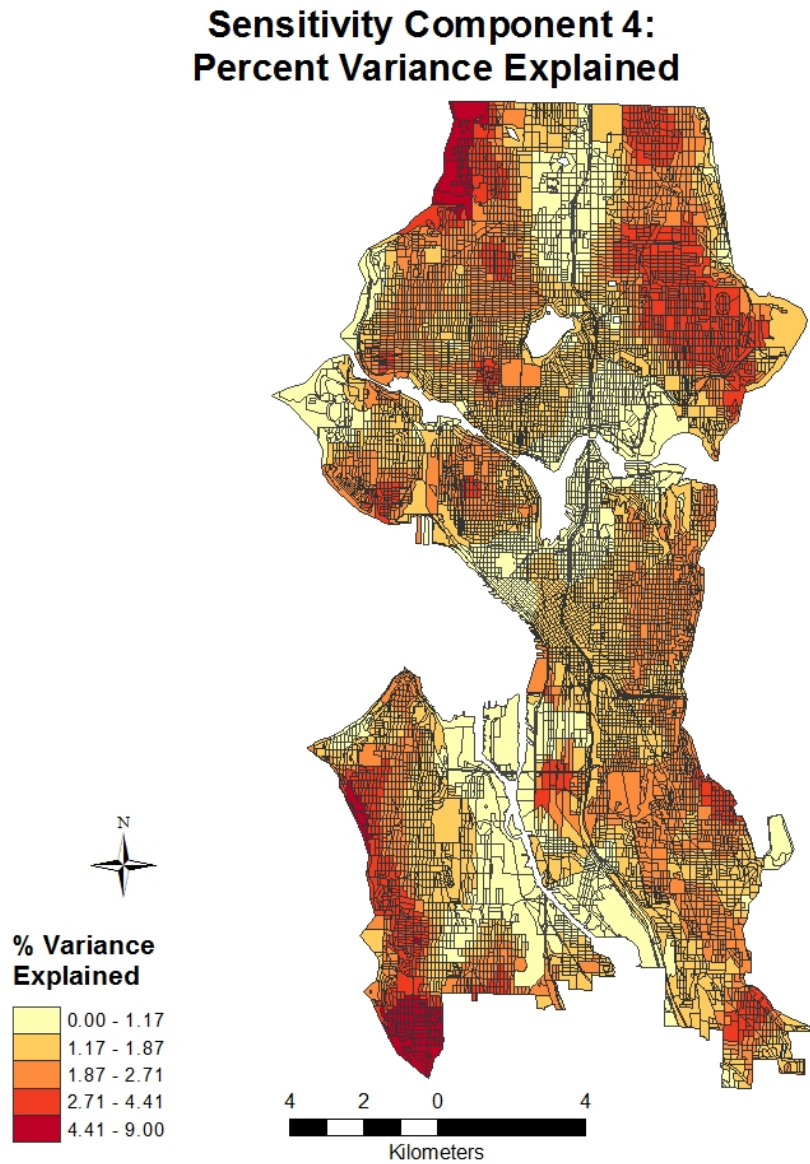


**Figure 31: GWSERV: Sensitivity Component 4 PVE map**

Figure 32 shows the deviation of the calculated sensitivity scores from the mean. Dark red represents higher levels of sensitivity and blue represents low levels of sensitivity. In this case, blocks with low sensitivity are located next to blocks with high sensitivity. This could indicate that there are often rapid changes between populations in different census blocks causing differences in sensitivity. There are few blocks with average sensitivity and most blocks have low sensitivity. As with the SERV sensitivity results, areas that are more exposed to SLR are less sensitive to it, however because of increased exposure and lower adaptive capacity they will be more vulnerable.

## GWSERV: Sensitivity Results

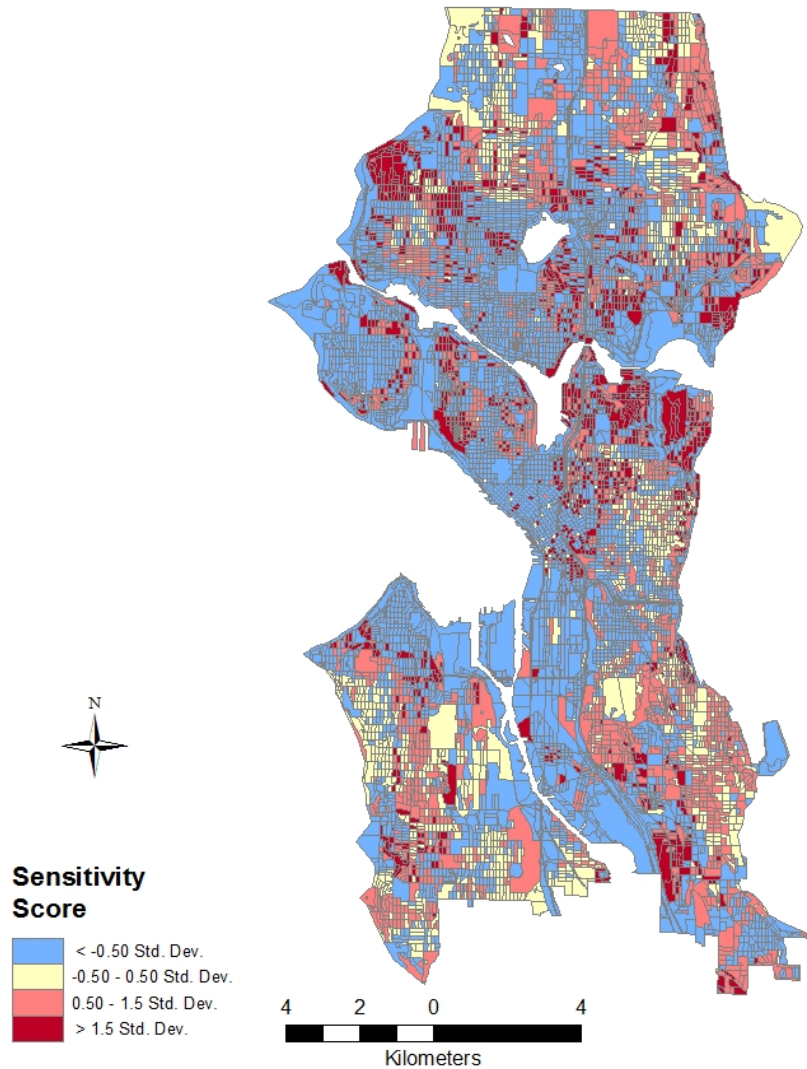


**Figure 32: GWSERV: Sensitivity Results map**

Figures 33, 34, 35, and 36 show the GWSERV score for Seattle with 0.010 m, 0.105 m, 3.804 m and 4.610 m of SLR. Areas of dark blue indicate lower vulnerability, whereas areas of dark red indicate higher levels of vulnerability. The results indicate that in most cases, the areas with the highest vulnerability are those with the most exposure. Most of the

census blocks are within 1.5 standard deviations of the mean. This indicates that a few blocks are very resilient, but are not exposed and those that are not exposed are no more or less vulnerable than other blocks that aren't exposed. There are sharp distinctions between very vulnerable areas and not vulnerable areas; this indicates that the blocks may have specific variables that make them more or less vulnerable. However, unlike the SERV results, there are no areas that are generally more or less resilient. This indicates that there is some spatial variability that is not accounted for in the SERV model.

**SLR Scenario: 0.010 (m)**  
**GWSERV**

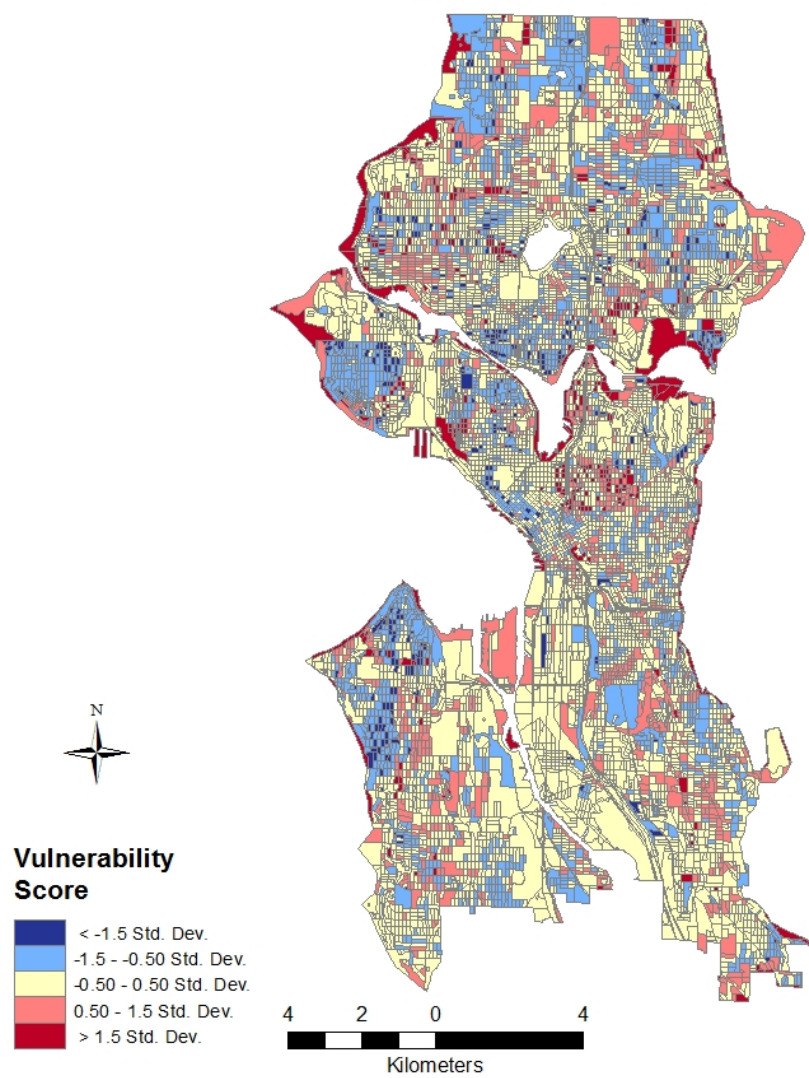


**Figure 33: GWSERV: 0.010 map**

### SLR Scenario: 0.105 (m) GWSERV

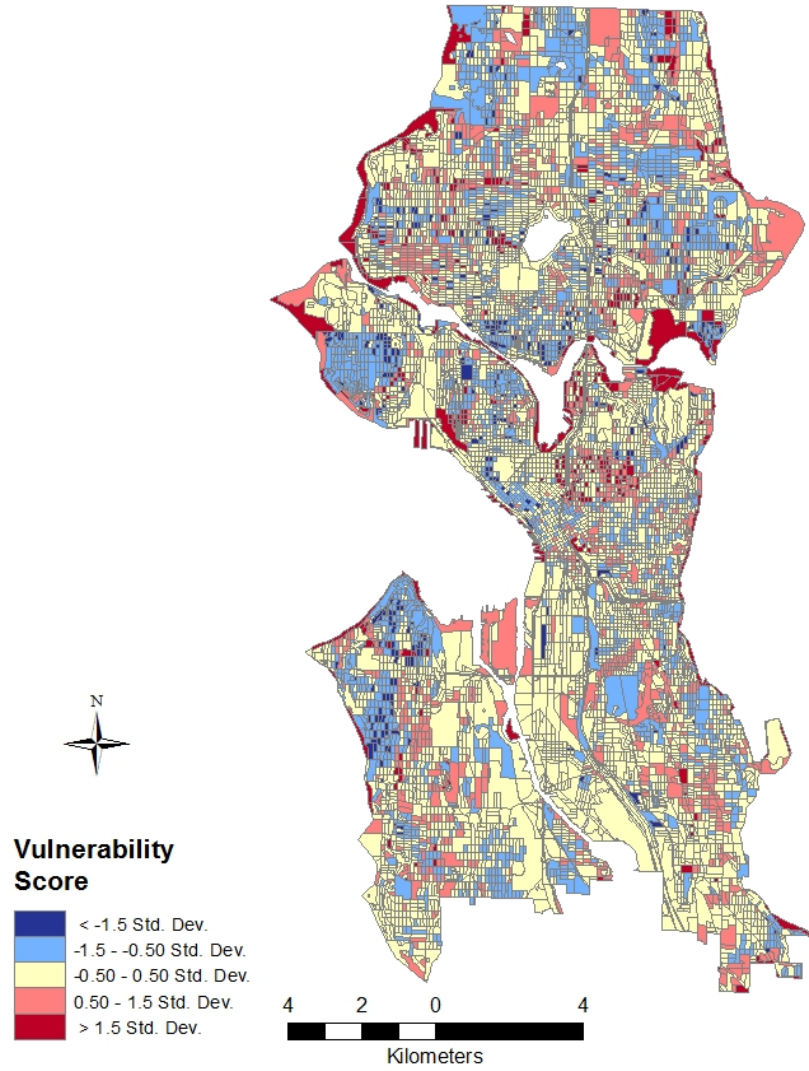
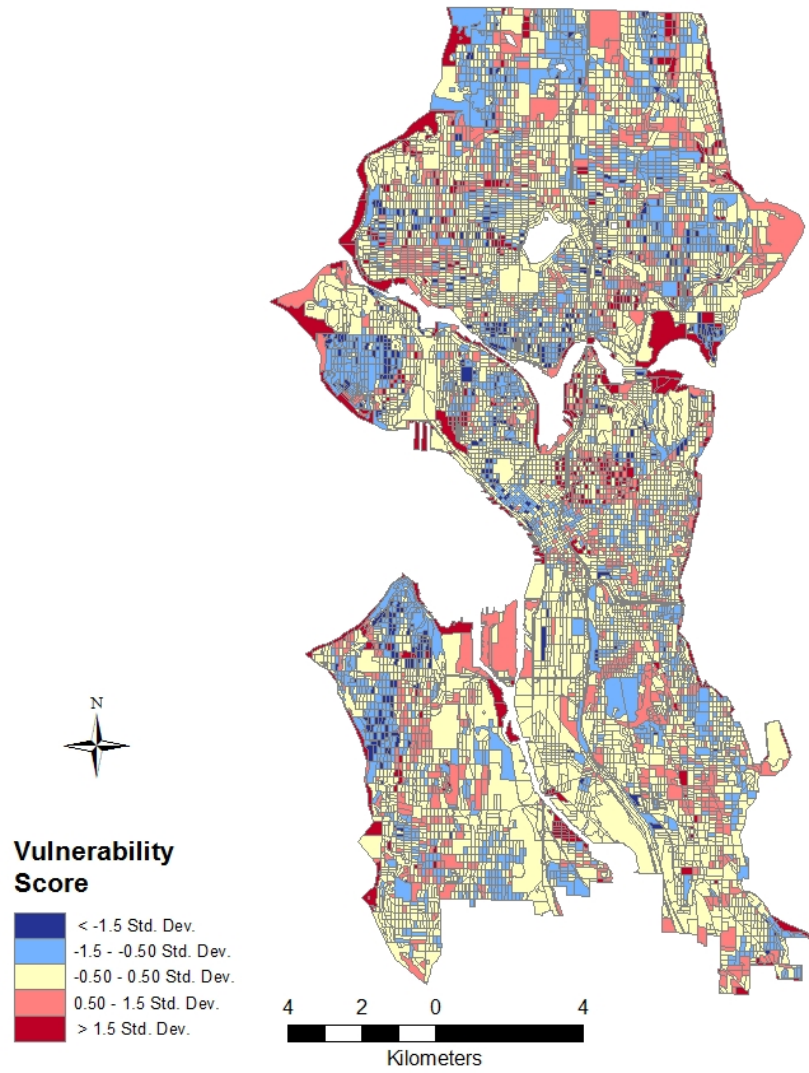


Figure 34: GWSERV: 0.105 map

**SLR Scenario: 3.804 (m)**  
**GWSERV**



**Figure 35: GWSERV: 3.804 map**

**SLR Scenario: 4.610 (m)**  
**GWSERV**

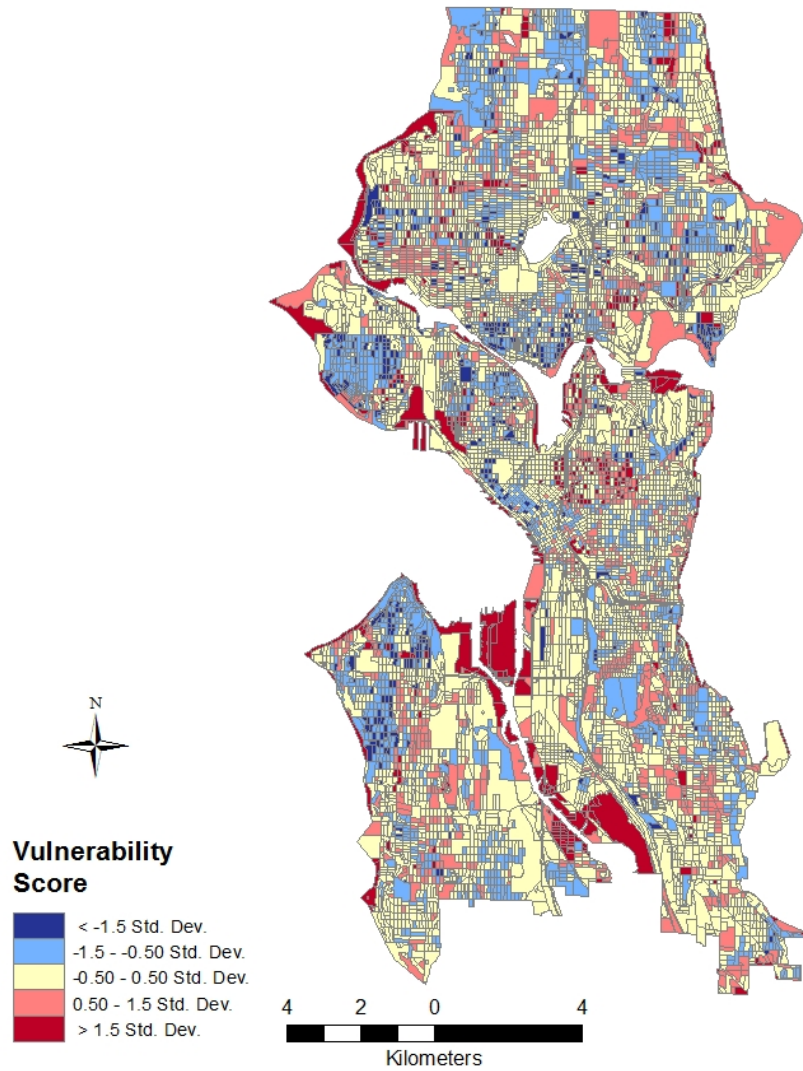


**Figure 36: GWSERV: 4.610 map**

### 3.4: SERV vs. GWSERV

The results from the SERV and GWSERV models were compared by counting the number of census blocks in each vulnerability bracket shown in table 7. The comparison was inconclusive, however some patterns emerged. For example, in each case, the GWSERV model had the highest number of blocks (shaded cells) in the lowest and average bracket. This suggests that the SERV model may be identifying a higher number of blocks with higher vulnerability.

<b>Count in each Vulnerability Bracket</b>					
	<b>Lowest</b>	<b>Low</b>	<b>Average</b>	<b>High</b>	<b>Highest</b>
<b>GWSERV 0.010</b>	384	2041	6867	1387	488
<b>SERV 0.010</b>	53	3396	5564	1419	735
<b>GWSERV 0.105</b>	384	2041	6867	1387	488
<b>SERV 0.105</b>	53	3396	5564	1419	735
<b>GWSERV 3.804</b>	438	2006	6813	1380	530
<b>SERV 3.804</b>	62	3415	5511	1421	758
<b>GWSERV 4.610</b>	516	1959	6711	1393	588
<b>SERV 4.610</b>	72	3460	5409	1424	802

**Table 7: Count in each Vulnerability Bracket**

### 3.5: Discussions and Conclusions

Social vulnerability and resilience measures can be used to direct hazard mitigation, adaptation, and recovery dollars and efforts to the areas that are least resilient and most vulnerable (Cutter, 1996; Cutter et al., 2008b; Frazier, Thompson, & Dezzani, 2013a). However, a community's vulnerability and resilience to a disaster will change depending on the exposure to the disaster as well as changing demographics. For example SLR threatens coastal populations with inundation during storms and high tide. High levels of SLR and inundation may make a community more vulnerable to inundation.

Traditional vulnerability models do not take into account spatial factors. However the SERV model and the GWSERV model do. Including spatial effects allows vulnerability models to more closely represent reality. Results of this study indicate that estimated SLR will have little impact on Seattle's vulnerability and resilience to inundation from SLR and high tide events. Here, 18 scenarios are considered, ranging between 0.01 and 4.61 m of SLR. The rapid change in elevation along the coast, from 0 m to 159 m (see Figure 37), could explain why SLR will affect only a small portion of Seattle. Lower lying communities will see more drastic changes in exposure and thus vulnerability and resilience (Frazier, Thompson, & Dezzani, 2013a). The SERV and GWSERV models indicate similar results (Figure 38); areas that have higher exposure are more vulnerable but there is little difference between 0.010 m and 4.610 m of SLR.

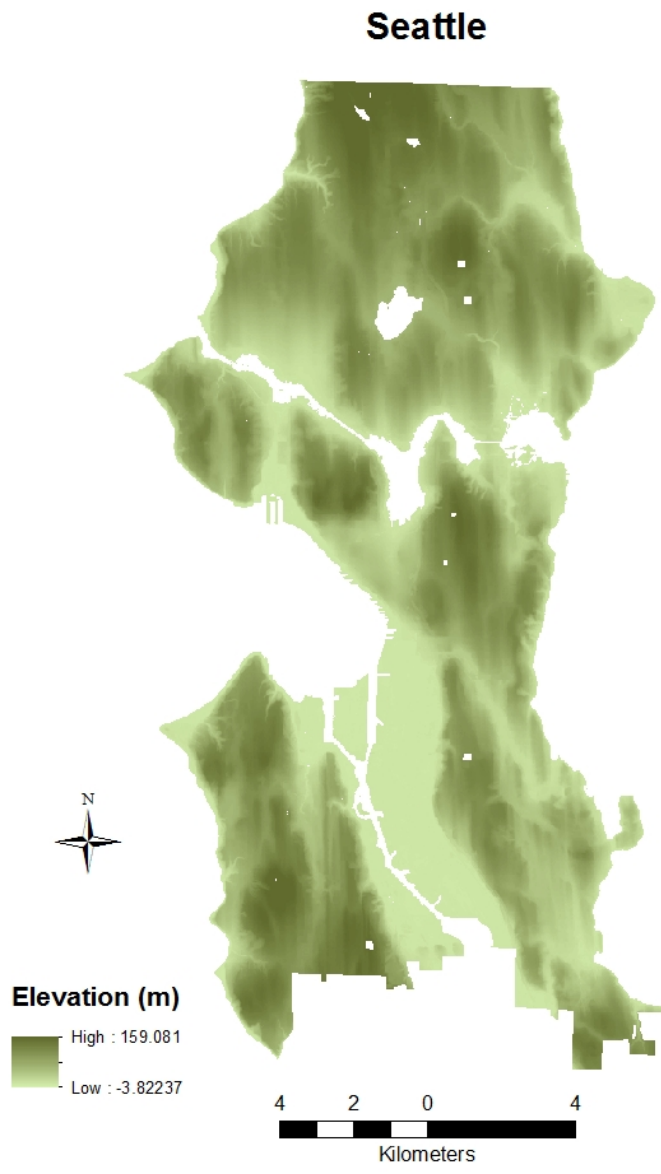


**Figure 37: Seattle Elevation**

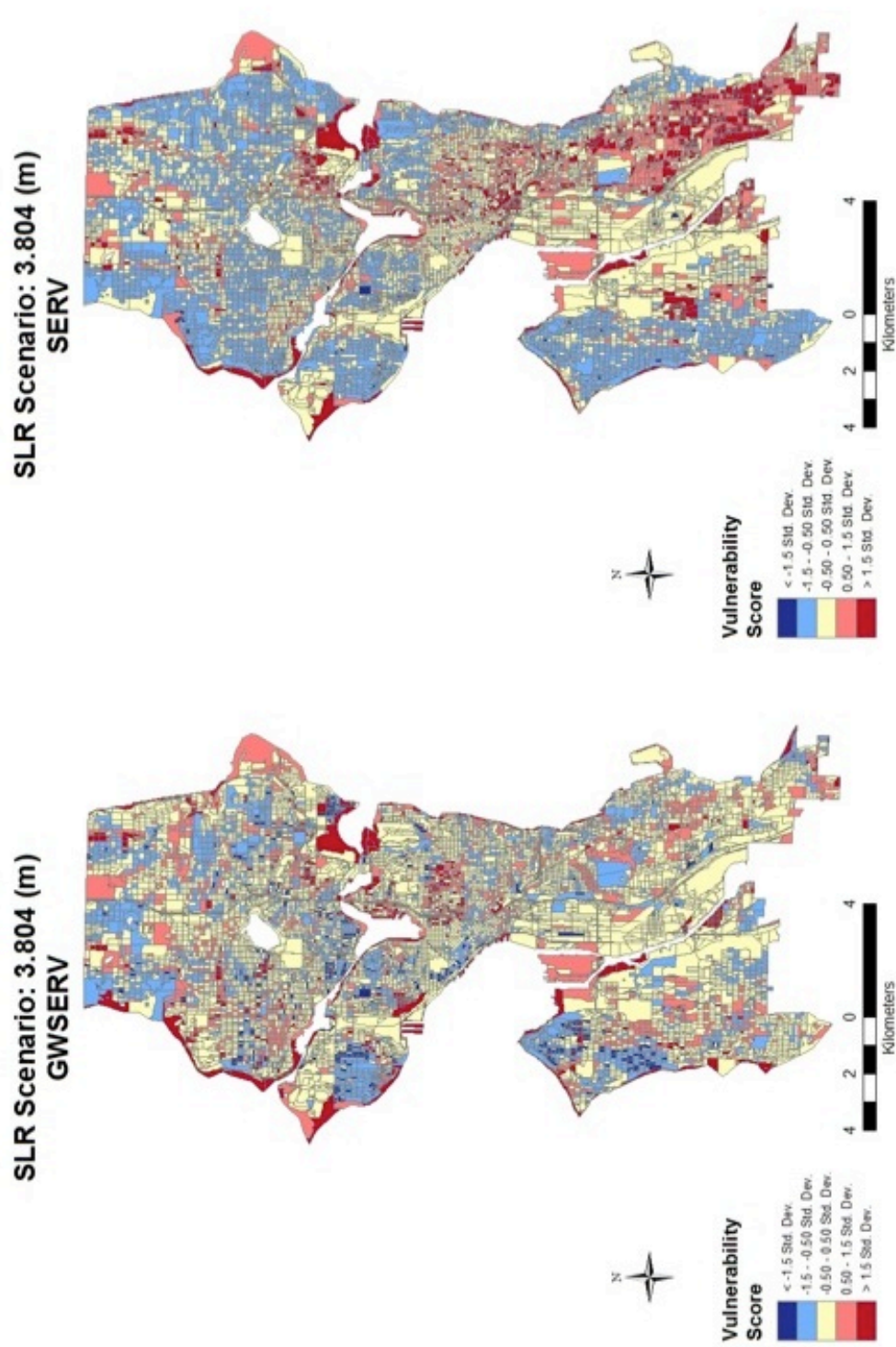


Figure 38: 3.804 Comparison

Although the same exposure scores were used in both the SERV and GWSERV models, the relative sensitivity and adaptive capacity scores were different. The SERV model works to integrate spatial autocorrelation between the census blocks into the PCA used in the model by including the Moran's I of the variables (a measure of spatial autocorrelation). On the other hand, the GWSERV model includes spatial effects by adding a geographic weight to the PCA in the model. Despite these differences, the two models provide statistically identical results when comparing the means. These statistical similarities are expected because each component (exposure, adaptive capacity, and sensitivity) of each model was transferred to a Z-score. Transforming values to Z-scores allows for combination of values with different units. However, this also forces scores to have identical means of zero.

Differences between GWSERV and SERV can be determined by comparing maps of the 3.804 m scenario in Figure 38. For example, the GWSERV map in Figure 38 shows that most of Seattle's vulnerability scores are within 0.50 standard deviations. The areas with the highest vulnerability are also the areas with the highest amount of exposure (see Figure 37). On the other hand, the SERV map in figure 38 indicates that most of the census blocks have a score that is not within 0.50 standard deviations. In the SERV model, both areas with no exposure and areas with exposure are very vulnerable. Although the SERV and GWSERV maps show different distributions of vulnerability, there are very few, if any, blocks that vary by more than one vulnerability bracket in either direction on either map. This indicates that both model are succeeding in showing the areas of high or low vulnerability.

Another explanation for the differences between the SERV and GWSERV models is that the GWSERV model might identify local outliers more consistently than the SERV

model because it directly calculates the effect of the surrounding blocks. The GWSERV model assumes that each block's neighbors has a higher impact on that block than the SERV model, making outliers stand out more. Essentially, the GWSERV model calculates individual PCA for each block while taking into account the neighboring blocks. On the other hand, the SERV model calculates one PCA for the whole study area. Future research will work to explain the differences in the two models and determine which is more accurate in different locations.

A benefit to using the GWSERV model is that it allows for stakeholders to determine which component and variable for each block is most important. For example, in some blocks homeownership is the largest component in adaptive capacity and other blocks it is race. This allows for stakeholders to better target ways to increase adaptive capacity in each block by counteracting the historical lack of agency for non-homeowners. The SERV model only provides the leading components for the entire study area, not a single block. The leading components are also not broken down into which variables have the highest impact within that component. This makes it more difficult for stakeholders to target specific aspects of vulnerability. The SERV model makes it possible to locate which blocks may need attention, but not which variables have the largest impact on sensitivity and/or adaptive capacity.

Although the GWSERV model accounts for more spatial variation than the SERV model with more detailed results, it does have some drawbacks. First, the model is more computationally intensive than the SERV. For example, the GWPCA adaptive capacity and sensitivity scores each took over 200 times longer to run than the PCA in the SERV model. Calculating the GWPCA can be difficult and requires one to find or write a script that does

so. For example at the time of this study, only 2 examples of calculated GWPCA were available. One was calculated using Fortran 77 code that was written by Lloyd 2010 and the other did not specify how it was calculated however the methodology was clear (Harris et al., 2011; Christopher D. Lloyd, 2010). The GWModel did not become publicly available until July 2013 and has some drawbacks. The first of which is the GWmodel chooses the variable with the highest loading to be the first component, not the variable with the highest absolute value. For instance, if block A has variables including G and H and H has a loading of 2 and G has a loading of -3, the GWModel identifies H as the first component, not G even if G has more of an influence on the block. This error should be remedied in future research.

In order to use the GWModel, one must have a solid understanding of how to write script within the statistics program R. Learning how to use R can be a difficult process and in many cases mistakes are not noticed until after the lengthy model run is completed. For example, the GWModel included an option to retain differing numbers of variables in the GWPCA results. However, this option was not properly written and after testing it multiple times, it did not work. In many cases the occupying GWModel manual was incorrect, contradictory, or vague. Because of this, time must be spent testing and changing different scripts to avoid errors. In order to write a script, one must be very fluent in the chosen computer language. Before the GWModel was available, the researcher was working to find ways to calculate the geographic weights and integrate that into a PCA. Because very few programs allow the geographic weights to be exported, this challenging task was abandoned when the GWModel was available.

Second, the bandwidth selection can be arbitrary. In this study, the bandwidth was calculated using the GWPCA bandwidth function included in the R Package. This research

calculates bandwidth with a Gaussian kernel and a goodness of fit model, however this may not always be the case. The bandwidth could be set to anything, changing the results. For example, Lloyd 2010 used only distance to determine the bandwidth instead of distance and number of nearest neighbors (C. D. Lloyd, 2012). Another drawback is that there is not yet an easy way to calculate eigenvalues in the GWModel. Although this is not necessary for the GWPCA, it can be useful to compare the results to the PCA.

Although there are drawbacks to using the GWSERV model, it provides a stakeholders with a better idea of where to target recovery and mitigation efforts and how to best direct those efforts making it more useful than the SERV model. Because the GWSERV model better incorporates the effect of neighboring blocks on each block, it is better able to show local outliers. In this case the outliers are the blocks that are in most need of assistance. The GWSERV also provides stakeholders with variable that has the most effect on the block, thus allowing the stakeholders to better target their efforts. The SERV model gives a good overview of areas that are more or less vulnerable, however it also identifies global, not local outliers making it harder for stakeholders to target efforts. The SERV model is a good way to identify areas of low or high vulnerability, however the GWSERV model shows areas that have low or high vulnerability as well as the appropriate variable to target to increase relative vulnerability.

Future research should focus on using more accurate and finer resolution DEMs to calculate SLR as well as including precipitation data, current flood plains, and stormwater conduit data into the analysis. It would also be beneficial to find a way to make SERV and GWSERV models temporal. Future research can also find ways to compare the SERV and GWSERV model (like the chi-square test) and find ways to test the accuracy of the models.

Another unanswered question is the effect of using correlated data to calculate sensitivity and adaptive capacity. More research can be done to estimate the amount of correlation between the two sets of variables and how to counteract that. More research may also be done in the GWSERV to see what the results are if one excludes different variables. Future work can also use the SERV or GWSERV to determine areas that are more or less vulnerable to other, more relevant hazards to Seattle, like earthquake damage or tsunami damage.

The research concluded that SLR will have very little impact on the vulnerability and resilience of Seattle. The benefits of using localized spatial analysis techniques in the development of resilience quantification frameworks are that the results provide more detailed and localized information. The constraints of localized spatial analysis are choosing an appropriate bandwidth, computation time, and script errors.

## References

- Adger, W. N. (2006). Vulnerability. *Global Environmental Change*, *16*, 268–281.  
doi:10.1016/j.gloenvcha.2006.02.006
- Bernstein, L., Bosch, P., Canziani, O., Chen, Z., Christ, R., & Davidson, O. (2007). Climate Change 2007: Synthesis Report, (November), 1–52.
- Birkmann, J. (2007). Risk and vulnerability indicator at different scales: Applicability, usefulness and policy implications. *Environmental Hazards*, *7*, 20–31.
- Broad, G., Campbell, D., Frazier, T., Howe, P., & Murtinho, F. (2010). Visualization of Slow-Developing Hazards: Influencing Perceptions and Behaviors to Facilitate Adaptation Planning. *Pan-American Advanced Studies Institute for the Integration of Research on Climate Change and Hazards in the Americas*, (July), 1–20.
- Burton, I., Kates, R. W., & White, G. F. (1978). *The environment as hazard* (p. 290). New York: Oxford University Press. Retrieved from  
[http://books.google.com/books?hl=en&lr=&id=8aK1YcbL5\\_8C&pgis=1](http://books.google.com/books?hl=en&lr=&id=8aK1YcbL5_8C&pgis=1)
- Charlton, M., Brunson, C., Demšar, U., Harris, P., & Fotheringham, A. S. (2010). Principal Components Analysis: from Global to Local. In *13th AGILE International Conference on Geographic Information Science 2010* (pp. 1–10). Guimarães, Portugal.
- Committee on Sea Level Rise in California, Oregon, and W., Resources, B. on E. S., Board, O. S., & Division on Earth and Life Studies. (2012). *Sea-Level Rise for the*

*Coasts of California, Oregon, and Washington: Past, Present, and Future. National Academies Press* (pp. 1–201).

Cooper, H. M., Chen, Q., Fletcher, C. H., & Barbee, M. M. (2012). Assessing vulnerability due to sea-level rise in Maui, Hawai‘i using LiDAR remote sensing and GIS. *Climatic Change*. doi:10.1007/s10584-012-0510-9

Cutter, S. L. (1996). Vulnerability to environmental hazards. *Progress in Human Geography*, 20(4), 529–539. doi:10.1177/030913259602000407

Cutter, S. L., Barnes, L., Berry, M., Burton, C., Evans, E., Tate, E., & Webb, J. (2008a). *Community and Regional Resilience: Perspectives from Hazards, Disasters, and Emergency Management. CARRI Research Report 1* (p. 33).

Cutter, S. L., Barnes, L., Berry, M., Burton, C. G., Evans, E., Tate, E., & Webb, J. (2008b). A place-based model for understanding community resilience to natural disasters. *Global Environmental Change*, 18, 598–606.

Cutter, S. L., Boruff, B. J., & Shirley, W. L. (2003). Social Vulnerability to Environmental Hazards. *Social Science Quarterly*, 84(2), 242–261. doi:10.1111/1540-6237.8402002

Cutter, S. L., Burton, C. G., & Emrich, C. T. (2010). Disaster Resilience Indicators for Benchmarking Baseline Conditions. *Journal of Homeland Security and Emergency Management*, 7(1).

Cutter, S. L., & Emrich, C. T. (2006). Moral Hazard, Social Catastrophe: The Changing Face of Vulnerability along the Hurricane Coasts. *The Annals of the American*

*Academy of Political and Social Science*, 604, 102–112.

doi:10.1177/0002716205285515

Cutter, S. L., Mitchell, J. T., & Scott, M. S. (2000). Revealing the Vulnerability of People and Places: A Case Study of Georgetown. *Annals of the Association of American Geographers*, 90(4), 713–737.

Demšar, U., Harris, P., Brunson, C., Fotheringham, A. S., & McLoone, S. (2013). Principal Component Analysis on Spatial Data: An Overview. *Annals of the Association of American Geographers*, 103, 106–128.

Department of Economic and Social Affairs. (2011). *Population Distribution, Urbanization, Internal Migration and Development: An International Perspective* (p. 378).

Fekete, A. (2009). Validation of a social vulnerability index in context to river-floods in Germany. *Natural Hazards and Earth System Science*, 9(2), 393–403.

doi:10.5194/nhess-9-393-2009

Fekete, Alexander. (2011). Spatial disaster vulnerability and risk assessments: challenges in their quality and acceptance. *Natural Hazards*, 61(3), 1161–1178. doi:10.1007/s11069-011-9973-7

Folke, C., Carpenter, S., Elmqvist, T., Gunderson, L., Holling, C. S., & Walker, B. (2002). Resilience and Sustainable Development: Building Adaptive Capacity in a World of Transformations. *AMBIO: A Journal of the Human Environment*, 31(5), 437–40.

Retrieved from <http://www.ncbi.nlm.nih.gov/pubmed/12374053>

- Fotheringham, A. S., Brunson, C., & Charlton, M. (2002). *Geographically Weighted Regression: The Analysis of Spatially Varying Relationships* (1st ed., p. 269). West Sussex, England: John Wiley & Sons.
- Frazier, T. G., Thompson, C. M., & Dezzani, R. J. (2013a). Development of a Spatially Explicit Vulnerability-Resilience Model for Community Level Hazard Mitigation Enhancement. (C. A. Brebbia, Ed.) *Disaster Management and Human Health Risk III: Reducing Risk, Improving Outcomes*, 133, 13–24.
- Frazier, T. G., Thompson, C. M., & Dezzani, R. J. (2013b). A Theoretical Framework for the Development of a Spatially Explicit Resilience-Vulnerability Model. *Annals of the Association of American Geographers*.
- Frazier, T. G., Thompson, C. M., Dezzani, R. J., & Butsick, D. (2013). Spatial and temporal quantification of resilience at the community scale. *Applied Geography*, 42, 95–107.
- Frazier, T. G., Wood, N., Yarnal, B., & Bauer, D. H. (2010a). Influence of potential sea level rise on societal vulnerability to hurricane storm-surge hazards, Sarasota County, Florida. *Applied Geography*, 30(4), 490–505. doi:10.1016/j.apgeog.2010.05.005
- Frazier, T. G., Wood, N., Yarnal, B., & Bauer, D. H. (2010b). Influence of potential sea level rise on societal vulnerability to hurricane storm-surge hazards, Sarasota County, Florida. *Applied Geography*, 30(4), 490–505. doi:10.1016/j.apgeog.2010.05.005

- Füssel, H.-M. (2006). Vulnerability: A generally applicable conceptual framework for climate change research. *Global Environmental Change*, *17*(2), 155–167.  
doi:10.1016/j.gloenvcha.2006.05.002
- Gallopín, G. C. (2006). Linkages between vulnerability, resilience, and adaptive capacity. *Global Environmental Change*, *16*, 293–303. doi:10.1016/j.gloenvcha.2006.02.004
- Godschalk, D. R., Brower, D. J., & Beatley, T. (1989). *Catastrophic Coastal Storms: Hazard Mitigation and Development Management*. Durham: Duke University Press.
- Haining, R. (2003). *Spatial Data Analysis: Theory and Practice* (1st ed., p. 452). Cambridge, UK: Cambridge University Press.
- Harris, P., Brunsdon, C., & Charlton, M. (2011). Geographically weighted principal components analysis. *International Journal of Geographical Information Science*, *25*(10), 1717–1736.
- Holling, C. S. (1973). Resilience and Stability of Ecological Systems. *Annual Review of Ecology and Systematics*, *4*, 1–24.
- Janssen, M. A., Schoon, M. L., Ke, W., & Börner, K. (2006). Scholarly networks on resilience, vulnerability and adaptation within the human dimensions of global environmental change. *Global Environmental Change*, *16*(3), 240–252.  
doi:10.1016/j.gloenvcha.2006.04.001
- Jolliffe, I. T. (2002). *Principal Component Analysis* (2nd ed., p. 518). New York, USA: Springer-Verlag.

- Kleinosky, L. R., Yarnal, B., & Fisher, A. (2006). Vulnerability of Hampton Roads, Virginia to Storm-Surge Flooding and Sea-Level Rise. *Natural Hazards*, 40(1), 43–70.  
doi:10.1007/s11069-006-0004-z
- Lloyd, C. D. (2012). Analysing the spatial scale of population concentrations by religion in Northern Ireland using global and local variograms. *International Journal of Geographical Information Science*, 26(1), 57–73.
- Lloyd, Christopher D. (2010). Analysing population characteristics using geographically weighted principal components analysis: A case study of Northern Ireland in 2001. *Computers, Environment and Urban Systems*, 34(5), 389–399.  
doi:10.1016/j.compenvurbsys.2010.02.005
- Lu, B., Harris, P., Gollini, I., Charlton, M., & Brunsdon, C. (2013). Package “GWmodel .”
- Mileti, D. S. (1999). *Disasters by Design* (1st ed., p. 351). Washington D.C: National Academy of Sciences.
- Morrow, B. H. (1999). Identifying and mapping community vulnerability. *Disasters*, 23(1), 1–18. Retrieved from <http://www.ncbi.nlm.nih.gov/pubmed/10204285>
- Mote, P. W., & Salathé, E. P. (2010). Future climate in the Pacific Northwest. *Climatic Change*, 102(1-2), 29–50. doi:10.1007/s10584-010-9848-z
- Mustafa, D., Ahmed, S., Saroch, E., & Bell, H. (2011). Pinning down vulnerability: from narratives to numbers. *Disasters*, 35(1), 62–86. doi:10.1111/j.0361

- Nie, L., Lindholm, O., Lindholm, G., & Syversen, E. (2009). Impacts of climate change on urban drainage systems – a case study in Fredrikstad, Norway. *Urban Water Journal*, 6(4), 323–332. doi:10.1080/15730620802600924
- Polsky, C., Neff, R., & Yarnal, B. (2007). Building comparable global change vulnerability assessments: The vulnerability scoping diagram. *Global Environmental Change*, 17, 472–485. doi:10.1016/j.gloenvcha.2007.01.005
- Saavedra, C., & Budd, W. W. (2009). Climate change and environmental planning: Working to build community resilience and adaptive capacity in Washington State, USA. *Habitat International*, 33(3), 246–252. doi:10.1016/j.habitatint.2008.10.004
- Schmidtlein, M. C., Deutsch, R. C., Piegorsch, W. W., & Cutter, S. L. (2008). A sensitivity analysis of the social vulnerability index. *Risk Analysis*, 28(4), 1099–1114. doi:10.1111/j.1539-6924.2008.01072.x
- Smit, B., & Wandel, J. (2006). Adaptation, adaptive capacity and vulnerability. *Global Environmental Change*, 16(3), 282–292. doi:10.1016/j.gloenvcha.2006.03.008
- Tate, E. (2012a). Social vulnerability indices: a comparative assessment using uncertainty and sensitivity analysis. *Natural Hazards*, 63(2), 325–347. doi:10.1007/s11069-012-0152-2
- Tate, E. (2012b). Uncertainty Analysis for a Social Vulnerability Index. *Annals of the Association of American Geographers*, (January 2013), 120820105450000. doi:10.1080/00045608.2012.700616

- Tate, E., Cutter, S. L., & Berry, M. (2010). Integrated multihazard mapping. *Environment and Planning B: Planning and Design*, 37(4), 646–663. doi:10.1068/b35157
- Thompson, C. M. (2012). *Development of a Probabilistic Storm Surge and Inland Precipitation Model and Theoretical Framework for Vulnerability and Resilience Quantification for Coastal Communities*. University of Idaho.
- Turner, B. L., Kasperson, R. E., Matson, P. A., McCarthy, J. J., Corell, R. W., Christensen, L., ... Schiller, A. (2003). A framework for vulnerability analysis in sustainability science. *Proceedings of the National Academy of Sciences of the United States of America*, 100(14), 8074–9. doi:10.1073/pnas.1231335100
- US Census. (2012). Seattle (city) QuickFacts from the US Census Bureau. Retrieved September 10, 2012, from <http://quickfacts.census.gov/qfd/states/53/5363000.html>
- US Department of Commerce National Oceanic and Atmospheric Administration. (2012). What percentage of the American population lives near the coast?? Retrieved September 10, 2012, from <http://oceanservice.noaa.gov/facts/population.html>
- Wisner, B., Blaike, P., Cannon, T., & Davis, I. (2004). *At risk: natural hazards, people's vulnerability and disasters* (2nd ed., p. 471). New York: Routledge. Retrieved from <http://books.google.com/books?id=566bdm7T5VEC&pgis=1>
- Wood, N. J., Burton, C. G., & Cutter, S. L. (2010). Community variations in social vulnerability to Cascadia-related tsunamis in the U.S. Pacific Northwest. *Natural Hazards*, 52(2), 369–389. doi:10.1007/s11069-009-9376-1

WTD. (2008). *Vulnerability of Major Wastewater Facilities to Flooding from Sea-Level Rise Tidally Influenced Facilities in King County's System.*

Wu, S.-Y., Yarnal, B., & Fisher, A. (2002). Vulnerability of coastal communities to sea-level rise: a case study of Cape May County, New Jersey, USA. *Climate Research*, 22, 255–270. doi:10.3354/cr022255